

Stratigraphy, palynology and organic geochemistry of the Devonian-Mississippian metasedimentary Albergaria-a-Velha Unit (Porto–Tomar shear zone, W Portugal)

Gil MACHADO, Eva FRANÇU, Milada VAVRDOVÁ, Deolinda FLORES,
Paulo Emanuel FONSECA, Fernando ROCHA, Luís C. GAMA PEREIRA, Alberto GOMES,
Madalena FONSECA and Helder I. CHAMINÉ



Machado G., Francú E., Vavrdová M., Flores D., Fonseca P. E., Rocha F., Gama Pereira L. C., Gomes A., Fonseca M. and Chaminé H. I. (2011) – Stratigraphy, palynology and organic geochemistry of the Devonian-Mississippian metasedimentary Albergaria-a-Velha Unit (Porto–Tomar shear zone, W Portugal). *Geol. Quart.*, **55** (2): 139–164. Warszawa.

The Albergaria-a-Velha Unit is one of several tectonostratigraphic out-of-sequence units of the metamorphic belt associated with the Porto–Tomar shear zone (Ossa–Morena Zone, W Portugal). It is composed of considerably deformed – very low grade – metasediments, namely shales, siltstones and rare fine sandstones. In this work we present new sedimentological and biostratigraphical data that suggest the Albergaria-a-Velha Unit was deposited from the (?)early Frasnian to the Serpukhovian in a distal marine environment, where turbiditic and basinal sedimentation prevailed. Palynofacies analysis and lithological data point to a gradual increase of terrestrial input, suggesting a prograding system. Detrital framework data is indicative of a stable cratonic sediment source area composed of low grade metamorphic rocks. The timing of the onset of the Porto–Tomar shear zone activity and consequently its influence on the sedimentation of this unit is discussed. Organic petrology and geochemistry data indicate that the Albergaria-a-Velha Unit is within the dry gas window in terms of hydrocarbon generation ranges.

Gil Machado, Centre GeoBioTec Universidade de Aveiro, 3810-193 Aveiro, Portugal, e-mail: machadogil@gmail.com; tavares.rocha@ua.pt; Eva Francú, Laboratory of Organic Geochemistry, Czech Geological Survey, Leitnerova 22, 658-69 Brno, Czech Republic, e-mail: eva.francu@geology.cz; Milada Vavrdová, Institute of Geology, Academy of Sciences of the Czech Republic, Rozvojová 269, 165-00 Praha 6, Czech Republic, e-mail: vavrdova@gli.cas.cz; Deolinda Flores, Department of Geosciences, Environment and Spatial Planning and Centre of Geology of University of Porto, R. Campo Alegre 687, 4169-007 Porto, Portugal, e-mail: dflores@fc.up.pt; Paulo Emanuel Fonseca, Department of Geology and Centre of Geology of the University of Lisbon (CeGUL), Faculty of Sciences of the University of Lisbon, Ed. C6, Campo Grande, 1749-016 Lisbon, Portugal, e-mail: pefonseca@fc.ul.pt; Fernando Rocha, Centre GeoBioTec Universidade de Aveiro, 3810-193 Aveiro, Portugal, e-mail: luis.gama@ua.pt; Luís C. Gama Pereira, Department of Earth Sciences and Centre of Geophysics of the University of Coimbra, Faculty of Sciences and Technology of Coimbra, Largo Marquês de Pombal, 3000-272 Coimbra, Portugal, e-mail: gpereira@dct.uc.pt; Alberto Gomes, Department of Geography, Faculty of Arts of the University of Porto and Centre of Geography and Territory Planning Studies Via Panorâmica s/n 4150-564 Porto, Portugal, e-mail: atgomes@netcabo.pt; Madalena Fonseca, Instituto de Investigação Científica Tropical, DCN-Geodes Tapada da Ajuda, 1349-017 Lisbon, Portugal, e-mail: madfons@isa.utl.pt; Helder I. Chaminé, Laboratory of Cartography and Applied Geology School of Engineering (ISEP), Polytechnic of Porto (ISEP), R. Dr. António Bernardino de Almeida 431, 4200-072 Porto, Portugal; Centre GeoBioTec Universidade de Aveiro, 3810-193, Aveiro, Portugal (received: January 16, 2011; accepted: June 14, 2011).

Key words: Mississippian, Late Devonian, Ossa–Morena Zone, Porto–Tomar shear zone, palynology, organic geochemistry.

INTRODUCTION

The Iberian Massif, in its northwestern region, is transected by a NNW–SSE major dextral deep-crustal shear zone, separating the Ossa–Morena Zone (OMZ) and the Central Iberian Zone – CIZ (e.g., Gama Pereira, 1987; Dias and Ribeiro, 1993; Chaminé *et al.*, 2003a; Ribeiro *et al.*, 2007, 2010). The

Porto–Tomar shear zone (PTSZ), in its northern sector, comprises a narrow metamorphic belt that extends from the Tomar area (western-central Portugal; Gama Pereira, 1987, 1998; Pereira *et al.*, 1998) to south of Porto area (NW Portugal; Chaminé, 2000; Chaminé *et al.*, 2003a, b). The general dextral sense of movement of this shear zone was considered to have started during the “Westphalian”, based on the tectono-sedimentary control of the Gzhelian (late Pennsylvanian)

intramontane Buçaco Basin (e.g., Lefort and Ribeiro, 1980; Ribeiro *et al.*, 1980; Gama Pereira *et al.*, 2008; Pinto de Jesus *et al.*, 2010), but Dias and Ribeiro (1993), using structural data from the CIZ, reinterpreted it as being already active since the Late Devonian early stages of the Variscan orogeny. The post-Mesozoic geodynamic evolution of Iberia has been dominated by reactivated inherited crustal structures, which have induced stress activity along the PTSZ segments from the end of the Variscan orogeny until the present-day (e.g., Gomes *et al.*, 2007; Gomes, 2008; de Vicente and Vegas, 2009).

The PTSZ metamorphic belt comprises several relative autochthonous and parautochthonous tectonostratigraphic units with high to very low metamorphic degrees, as well as allochthonous units of medium to high metamorphic grades (Severo Gonçalves, 1974; Gama Pereira, 1987, 1998; Chaminé, 2000; Chaminé *et al.*, 2003a, b; Fernández *et al.*, 2003, and references therein). The Albergaria-a-Velha upper Paleozoic metapelitic rocks were initially reported by Chaminé (2000) and later named the Albergaria-a-Velha Unit (AVU) by Chaminé *et al.* (2000). This is one of several tectonostratigraphic out-of-sequence units, related to partition of crustal deformation, of the PTSZ metamorphic belt (Chaminé, 2000). The first palynological data published by Fernandes *et al.* (2001) and Chaminé *et al.* (2003a) suggest depositional ages far it of between Late Devonian and Mississippian. The AVU is tectonically imbricated with a garnetiferous black-greenish metapelitic unit of late Proterozoic age (Beetsma, 1995; Fernández *et al.*, 2003), the so-called Arada Unit, and its metapelitic equivalents further south to the region of Coimbra and Tomar (Gama Pereira, 1998; Chaminé *et al.*, 2003a, b), making the cartographic differentiation of the two units extremely difficult.

The AVU is overlain unconformably by Upper Triassic terrestrial deposits (Grés de Silves Fm. – Fig. 3A) of the Lusitanian Basin (Courbouliex, 1974; Palain, 1976; Gomes, 2008), but not by deposits of the Gzhelian Buçaco Basin (see Fig. 1). These have faulted contacts with the AVU and both are overlain unconformably by the Grés de Silves Fm. (Ribeiro, 1853).

Vázquez *et al.* (2007) examined the phyllosilicate crystallographic parameters of AVU samples which indicated maximum palaeotemperatures and pressures ranging from high anchizone to epizone, i.e., maximum temperatures >200°C and pressures between 1 and 2 Kbar

This work presents new data on the bio- and lithostratigraphy of the AVU and also on its hydrocarbon source rock potential and thermal history.

MATERIALS AND METHODS

LITHOSTRATIGRAPHY

Detailed sedimentological and stratigraphical description can only be performed on the few undeformed, relatively continuous sequences of coarser-grained metasedimentary rocks (see Fig. 1 for locations and Fig. 2 for sections). These were logged and sampled for palynology, thin sections and polished surfaces to observe relevant sedimentary features. All other

known localities may have a few relatively undeformed beds (<1 m thick), but are invariably bounded by faults and are usually folded (deformed under fragile-ductile or brittle-ductile conditions), making it impossible to properly describe and interpret the successions. The sand/mud ratio was visually estimated for each locality and groups of exposures, both highly deformed and relatively undeformed.

PALYNOLOGY

Several hundred dark grey and black shale and siltstone samples were collected. Of these *ca.* 250 were processed for palynology using a method similar to the one described by Ellin and McLean (1994). About 60 productive samples were used in this study (see Appendix C).

The slides produced were observed under a transmitted light microscope, at the GeoBioTec Research Centre of the University of Aveiro. The thermal alteration index (TAI) was visually estimated in all samples. Documentation of observable palynomorphs was conducted using an *Olym pusDP20* digital camera attached to an *Olym pusBX40* transmitted light microscope. Selected productive residues were mounted on acrylic plates, air-dried and observed (and photographed) using an *Olym pus C3030* digital camera attached to a reflected light *Olym pus BX60* microscope. Several oxidation methods were tested but none was effective. Due to the general poor quality of the organic residues obtained from the AVU the palynofacies analysis was limited to a few fundamental categories of palynomorphs. 30 samples of known age were used. For each sample, two types of analysis were performed:

1. Total particulate organic matter content analysis as observed on slides made from a non-sieved residue. Table 1 summarizes the categories considered.
2. Non-amorphous organic matter (AOM) analysis observed on slides produced from a 7 µm-sieved organic residue. Table 2 summarizes the categories considered.

Most categories can be easily recognized under transmitted light microscopy. Chitinozoans and zooclasts were grouped because their differentiation is often difficult due to the considerable maturity of the organic matter. Phytoclasts could be differentiated in most instances by their overall morphology. Smaller and heavily degraded particles that could not be positively identified were not counted.

SEDIMENT PROVENANCE

The AVU is composed essentially of pelitic metasediments. The 9 samples used in this work derive from rare fine sand-grade rocks forming the bases of turbidite beds (see Appendix C and Table 5). The samples were thin-sectioned preferentially parallel to bedding in order to obtain a homogenous grain-size within the thin section. 300 particles were counted in each thin section using a semi-automated Swift point counter coupled with a *Leitz Orthoplan* microscope. Observation and counting was performed with crossed polars. The Gazzi-Dickinson counting method was used (Gazzi, 1966 in Ingersoll *et al.*, 1984). Particles smaller than 0.00625 mm (silt-sized and

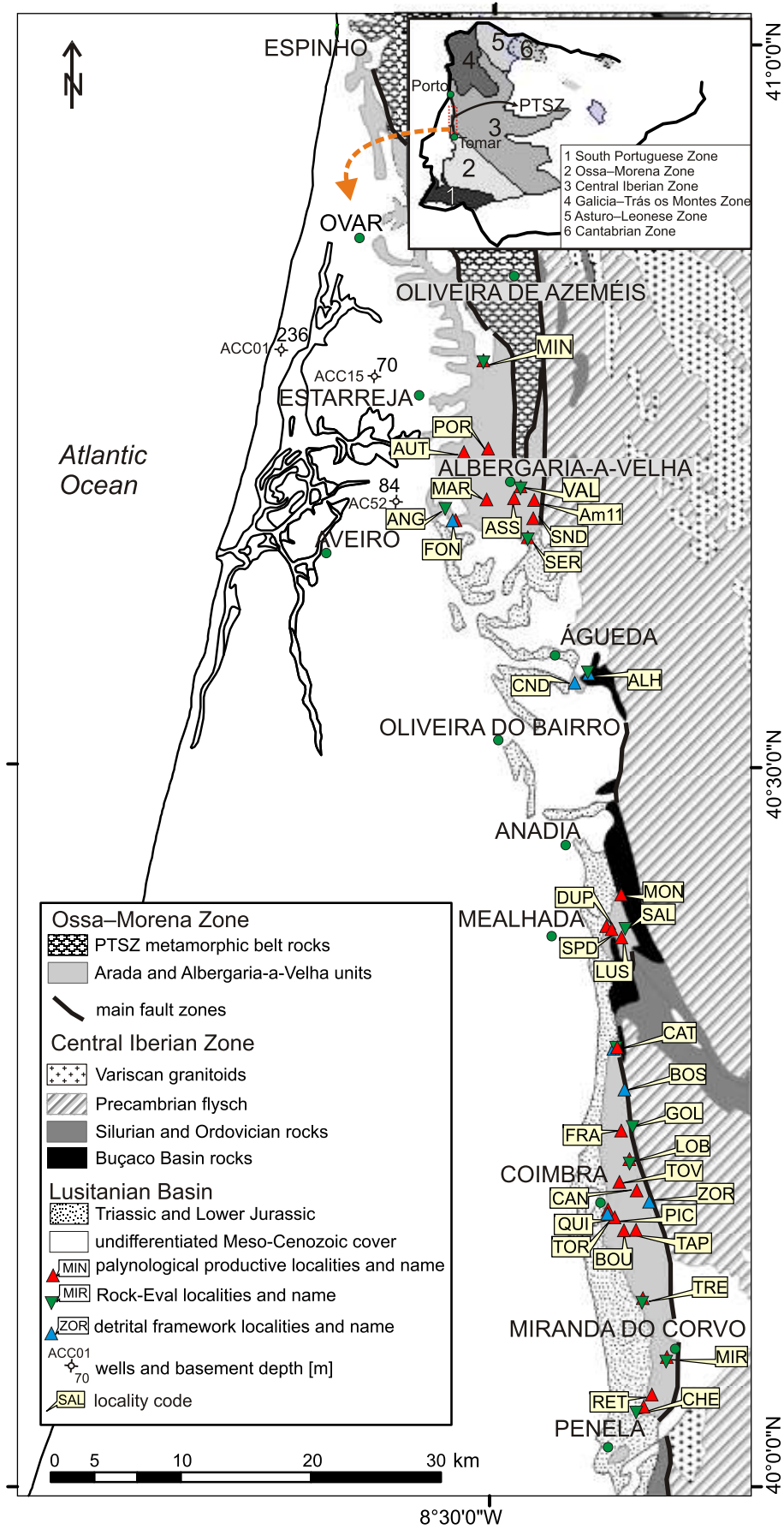


Fig. 1. Simplified geological map of the Espinho–Miranda do Corvo sector of the PTSZ metamorphic belt (adapted from Chaminié *et al.*, 2003a) with the localities studied (see Appendix C)

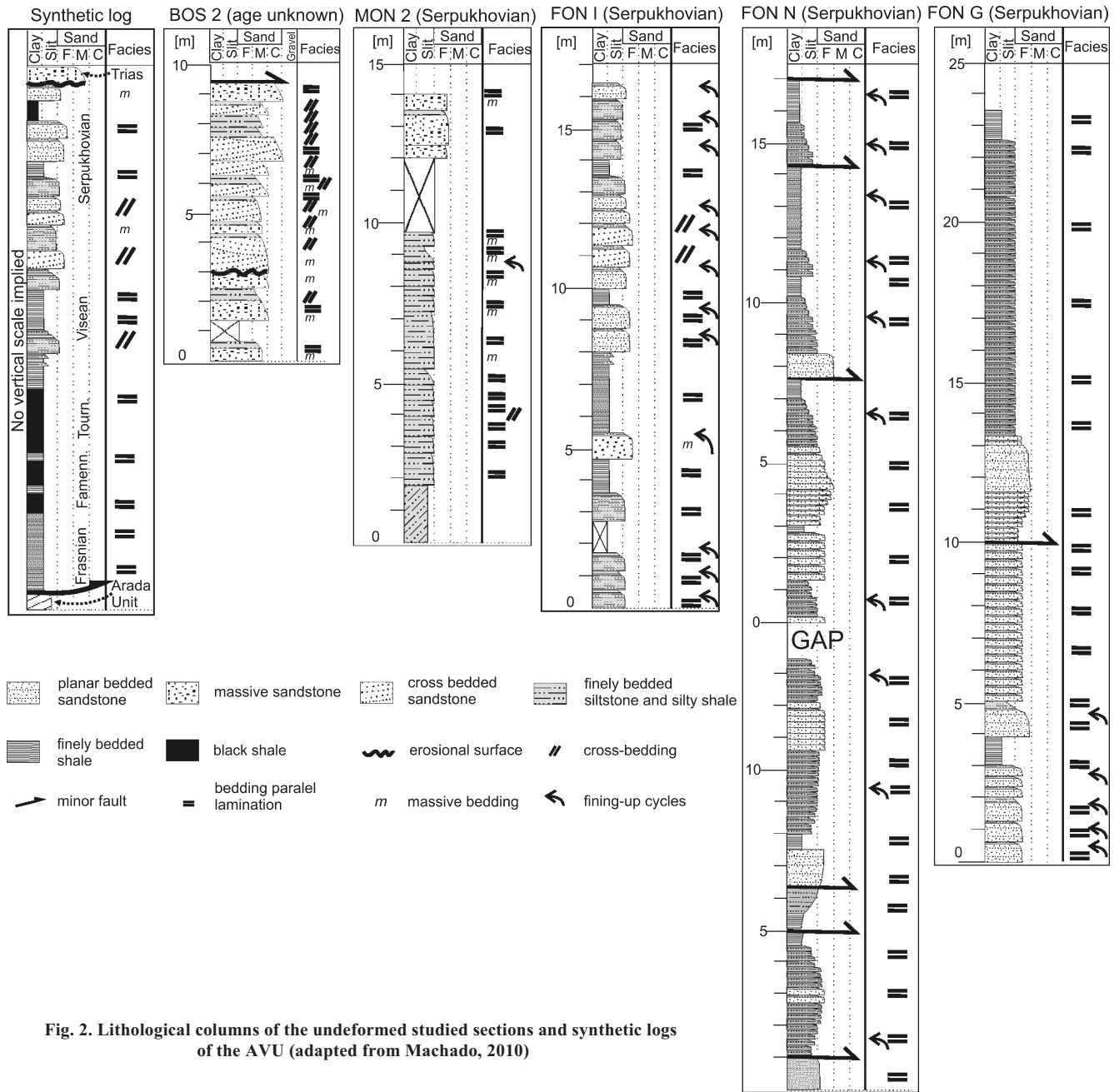


Fig. 2. Lithological columns of the undeformed studied sections and synthetic logs of the AVU (adapted from Machado, 2010)

Table 1

Summary table of the selected categories used for palynofacies analysis on non-sieved slides

Category	Palaeoenvironmental significance	Source rock
AOM	stratified water column or deep basin; anoxic-suboxic conditions	oil-prone
Phytoclasts	exclusively land-derived, proxy for shore proximity	gas-prone
Palynomorphs	variable	oil-prone

Compiled from Tyson (1987, 1993) and Batten (1996a, b)

smaller) were counted as matrix. Grains of doubtful origin (matrix recrystallization or silicification) were not considered. Table 3 summarizes the several categories of grains counted and some of their main characteristics.

Due to the low grade metamorphism and deformation, only 5 samples were suitable for counting the number of undulatory and non-undulatory quartz grains and also the number of crystals of each polymineralic quartz grain using the parameters defined by Basu *et al.* (1975).

The results were plotted on ternary diagrams and compared with previously defined fields (Basu *et al.*, 1975; Dickinson and Suczek, 1979; Dickinson *et al.*, 1983) using *Grapher 4.0* software.

Table 2

Summary table of the selected categories used for palynofacies analysis on 7 µm-sieved slides

Category	Origin	Palaeoenvironmental significance	Source rock
Spores	terrestrial	exclusively land-derived, proxy for shore proximity	oil-prone
Phytoclasts		exclusively land-derived, proxy for shore proximity	gas-prone
Zooclasts	marine	benthic marine arthropods, but also land derived debris	inert
Chitinozoans		exclusively marine, relatively deep environments	?
Acritarchs		exclusively marine, proxy for organic productivity under "normal" marine conditions	oil-prone
Prasinophytes		dominant in abnormal marine conditions (salinity, temperature, oxygenation, etc.)	highly oil-prone

Compiled from Tyson (1987, 1993), Miller (1996) and Batten (1996a, b)

Table 3

Grain categories considered for this study, their main characteristics and groups of grain categories used for ternary plots

Grains	Code	Main characteristics	
Quartzose monocrystalline	Qm	fresh, commonly with undulatory extinction pattern	
Quartzose polycrystalline	Qp	mostly chert grains, minor fine-grained quartzites	
Plagioclase	P	typically slightly weathered and small; characteristic polysynthetic twinning	
K feldspar	K	typically slightly weathered and small	
Undifferentiated feldspars	Fx	typically slightly weathered and small	
Lithic fragments	L	black, cryptocrystalline occasionally with very fine micas	
Dense minerals	D	very rare, mostly pyroxenes (?)	
Uncertain	Misc	too weathered of difficult to distinguish from matrix	
Matrix	M	generally siliceous, often with small micas	
Groups of grain categories considered for QFL and QmFLt ternary plots			
QFL	total quartz	Q	Qm + Qp
	feldspars <i>s.l.</i>	F	P + K + Fx
	lithic fragments	L	L
QmFLt	monocrystalline quartz	Qm	Qm
	feldspars <i>s.l.</i>	F	P + K + Fx
	total lithics	Lt	L + Qp

ORGANIC GEOCHEMISTRY AND VITRINITE REFLECTANCE

A total of 12 samples of dark grey to black shales were taken for organic geochemistry analysis (see Fig. 1 and Appendix C for the localities). The samples were gently pulverized, homogenized and sieved through a 1 mm mesh. All samples were subjected to elemental analysis of total organic and inorganic carbon using an *Eltra Metalyt CS 100/1000S* apparatus at the Laboratory of Organic Geochemistry of the Czech Geological Survey (Brno). Selected samples were analysed by *Rock-Eval 6* according to methodology described by Espitalié

et al. (1985) and Lafargue *et al.* (1998). The analyses were carried out in nitrogen at a programmed temperature of 300–550°C with heating rate of 25°C/min. Several organic geochemical parameters were obtained, namely S1 – free hydrocarbons (mg HC/g rock); S2 – bound (pyrolytic) hydrocarbons (mg HC/g rock); S3 – pyrogenic CO₂ and CO and peak temperature of pyrolysis (T_{max}); HI – hydrogen index (mg HC/g TOC) and OI – oxygen index (mg CO₂/g TOC).

Selected palynological residues obtained by cold HF dissolution of mineral matter were mounted using a method adapted from Hillier and Marshall (1988) and observed under a *Leitz OrthoPlan* (reflected light) microscope of the Organic Petrol-

ogy lab of the Department of Geosciences, Environment and Spatial Planning of the Faculty of Sciences of the University of Porto. Vitrinite reflectance measurements and photomicrographs were obtained with the image analysis software *Fos sil* and *Diskus*.

RESULTS

STRATIGRAPHY, SEDIMENTOLOGY AND FACIES

The sand/mud ratio varies greatly, but seems to be fairly similar within a group of exposures over areas of a few km². It varies between 0–100% to 80–20% and the total average, and also the mode, is close to 30–70%. The few undeformed sequences described in detail here are sandstone- and locally siltstone-dominated and thus have higher-than-average ratios. Very rare cm-thick oil shale beds can be observed in some sections. Macrofossils and trace fossils were not found.

The vast majority of non-weathered exposures had rocks of light to dark grey or black colour. Considering the localities where some sedimentary information could be obtained, three main types of lithofacies can be defined. These should be, however, considered end members of a continuum. The main characteristics are summarized in Table 4.

The laminated grey shale facies is very commonly observed and can be recognized even in considerably deformed rocks, as the striking contrast of light grey and dark grey mm-thick laminae is often preserved. The lamination is defined by darker and finer-grained laminae alternating with lighter and slightly coarser-grained laminae. This is observed at hand specimen and thin section scales (Fig. 3G).

The black shale facies can be found in localities which are entirely composed of shales (Fig. 3E) with an extremely reduced fine siltstone component – sand/mud ratio close to 0–100%. Pyrite is frequently observed at these localities. Lamination is faint and only seldom seen between very penetrative foliation planes.

The sand-silt-shale lithofacies is characterized by high sand/mud ratios (close to 80–20%). Short undeformed sequences belonging to this lithofacies allow the observation of characteristic cm- to dm-thick beds of sandstone or coarse

siltstone fining-upwards to finely laminated shales (Fig. 3B, C). Five sections assignable to this lithofacies were suitable for describing relatively continuous stratigraphic sequences (up to 24 m) and examining the details of sedimentary features (Fig. 2).

Sections FON I and FON G (see Fig. 2) are composed of dm- to m-thick (rarely cm-thick) successive beds of fining-upward cycles. Most beds are composed dominantly of siltstones that fine up to shales, but some fine sandstone-dominated beds also occur. These beds typically have a coarser, massive or crudely bedded base and a finer laminated top. Occasionally cross-beds can be observed in a cm- to mm-thick intermediate interval. These correspond to parts $a \pm c + d \pm e$ of Bouma sequences (Bouma, 1962). Within these sections, some intervals are composed solely of very fine siltstones and shales which can represent basinal deposition occurring between turbidity current events (level e of Bouma sequences). These sections are interpreted as a succession of low density turbidite beds.

Section FON N (Fig. 2) shows beds reflecting low-density turbidity currents. These are generally finer grained and the fining-upward cycles are not as well-defined and some beds show even reverse grading. Additionally some siltstone beds do not show significant changes in grain-size and lack the massive/cross bed/laminated sequence observed elsewhere. This type of succession of dm-thick fine sandstone and siltstone beds associated with thin shale beds is interpreted as a succession of low-density turbidites deposited in a considerably more distal setting interbedded with basinal sediments represented by the shale-dominated intervals; they might also represent pro-delta deposits not necessarily associated with turbidity currents.

The MON 2 section (Fig. 2) shows a sequence of siltstone-dominated turbidite beds with fairly regular thicknesses, although some very fine fining-upwards cycles can be observed (*ca.* 9 m). Cross-bedding is rarely observed, although this feature may be obscured by the substantial oxidation of this section. Most beds correspond to levels a and d of Bouma sequences. Level e (shales at the top of each cycle) is very poorly developed at this section.

A single section (BOS 2; see Fig. 2) shows dm- to m-thick fining-upward cycles that commonly have medium to coarse sand-grained bases that grade to siltstones and more rarely shales. At least in one of the cycles the base is defined by an erosive surface. Fairly complete Bouma sequences can be ob-

Table 4

Essential characteristics of the 3 end-members of the lithofacies defined for the AVU

Lithofacies	Description	Associated palynofacies (shales)	Stratigraphical occurrence	Interpretation
Laminated grey shales	grey shales with mm- to cm-thick darker and lighter laminae	very high AOM; acritarchs and prasinophytes rare, spores common	Frasnian to Serpukhovian	basinal sedimentation with seasonal control(?)
Black shales	black shales with minimal coarser or lighter material; lamination seldom visible	very high AOM; acritarchs and prasinophytes may be common; spores very common	essentially Famennian–early Tournaisian, but some Viséan and Serpukhovian occurrences	basinal sedimentation in anoxic conditions
Sand-silt-shale beds	successive cm- to m-thick beds with normal grading; massive base, laminated top, occasionally cross beds	few or none organic-walled microplankton; abundant spores; phytoclasts occasionally frequent	restricted to the Serpukhovian	low density turbidites and (?)pro-delta deposits

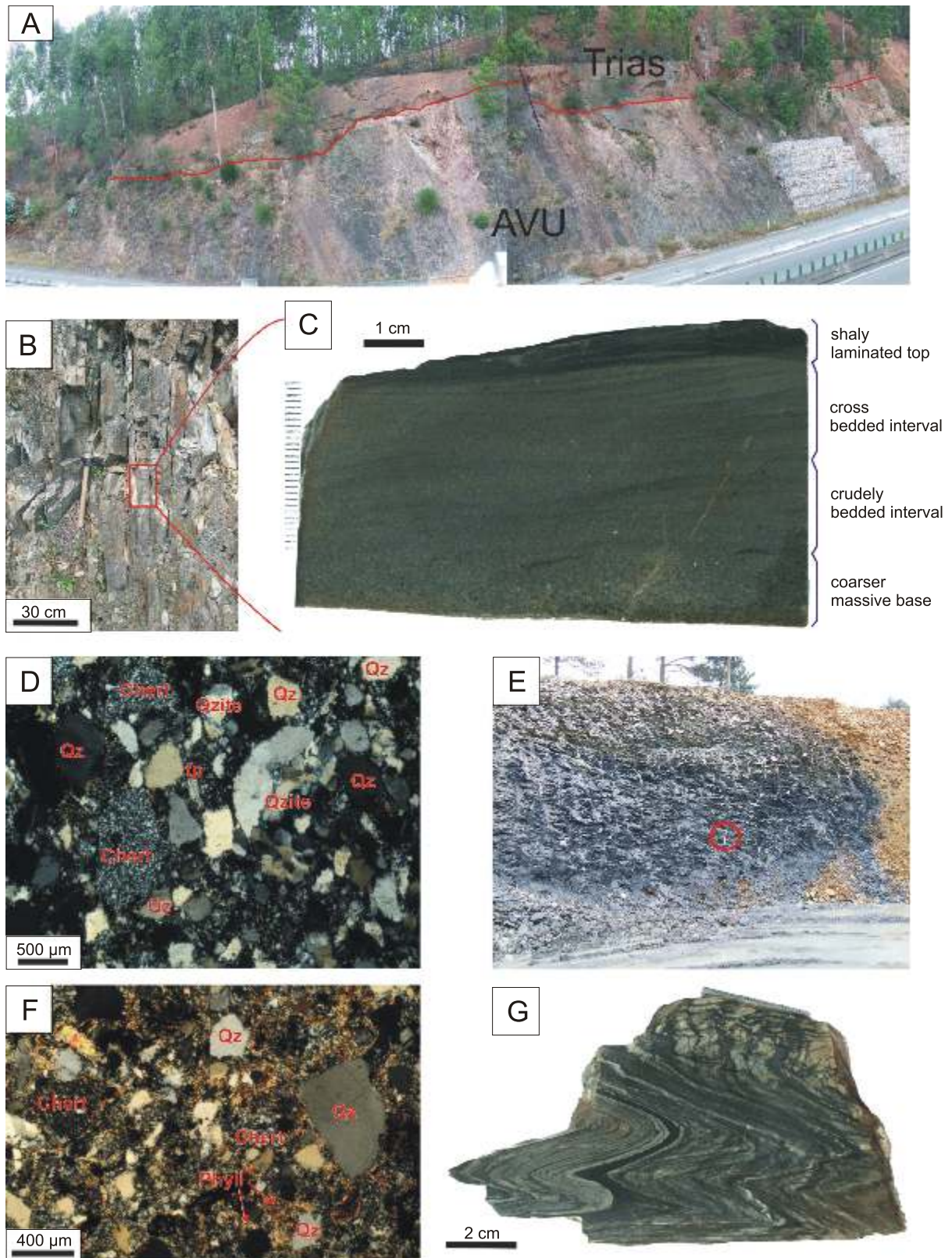


Fig. 3. Selected images of the AVU at the outcrop, hand sample and thin section scales

A – unconformity of the Upper Triassic strata over the AVU; note the intense ferruginization of the AVU; IP3 road, near Coimbra; **B** – outcrop with successive (near vertical) turbidite beds; way-up to left; sand-silt-shale lithofacies; ALH locality, near Águeda; **C** – detail of one of the beds from **B** showing one fining-upwards cycle; polished surface; **D** – photomicrograph of a thin section from the base of a turbidite bed; ALH locality near Águeda; crossed polars; **E** – fresh exposure of the black shale facies; ASS locality (near the type locality of Albergaria-a-Velha); hammer in red circle for scale; **F** – photomicrograph of a thin section from the base of a turbidite bed; BOS locality; note the metamorphic growth of phyllosilicates (multicolour tints) replacing the original cement/matrix; crossed polars; **G** – example of the finely laminated grey shale facies; polished surface; note the alternation of lighter, slightly coarser laminae and darker, finer laminae; SND locality, near Albergaria-a-Velha; fp – feldspar, Qz – quartz, Qzite – quartzite, Phyll – phyllosilicates

served, with a thick coarse massive base (level a), a crudely to well bedded interval of medium sands (level b), cross laminated sands (level c) and parallel laminated siltstone top (level d). Shales are seldom present at the tops of cycles.

DETRITAL FRAMEWORK ANALYSIS AND PROVENANCE

The absence of very coarse-grained metasediments in the AVU precludes direct and precise identification of transported grains and thus the identification of the sediment source areas. The collected point-counting data set shows that samples are all wackes, either quartz, sublithic or subarkose wackes, due to their high matrix/cement contents (see Table 5).

Quartz grains, mono- and polymineralic, (Qm + Qp) dominate all frameworks analysed, ranging from 64 to 95% of all grains (Table 5 and Fig. 3D, F). Undulatory extinction was commonly observed, although the extinction pattern differed

between grains, suggesting that the deformation episode that created the undulatory extinction affected rocks in the sediment source areas and not the AVU itself. Quartzite and chert grains (Qp) were frequently observed (1 to 22.3%; Fig. 3D, F). Feldspars *s.l.* (K + P + Fx) are quite rare (0 to 3.3%), considerably smaller than other grains and frequently weathered. Lithic fragments (L) are usually rare, ranging from 0 to 6%. These are in most instances black cryptocrystalline rocks, occasionally with very small mica crystals. They may be volcanic derived lithoclasts, but their true nature is uncertain.

One single sample group is visible, plotting in the craton interior and recycled (quartzitic) orogen fields (Fig. 4). The average modal composition of the sample group is $Q_{91.4}F_{2.9}L_{5.7}$ and $Qm_{76.5}F_{2.9}Lt_{20.6}$. The considerable proportion of polycrystalline quartz grains (Qp) accounts for the “shift” from the Qm corner (see Fig. 4).

All samples analysed were dominated by undulatory quartz (58 to 67% of all quartz grains). The proportions of non-undu-

Table 5

Framework modes, and classification of the sandstones from the AVU

Category	Qm [%]	Qp [%]	P [%]	K [%]	Fx [%]	L [%]	M [%]	D [%]	Misc [%]	Classification
Sample										
ALH3.3	51.7	11.7	0.0	0.0	0.3	2.0	32.3	0.7	1.3	quartz wacke
ALH3.2	52.3	22.3	1.0	0.0	0.7	3.3	18.3	0.3	1.7	quartz wacke
BOS3.2	35.7	13.0	1.0	0.0	0.0	6.0	39.0	1.7	3.7	(sub)lithic wacke
BOS4.1	36.0	6.0	0.0	0.0	0.0	6.0	47.3	2.7	2.0	(sub)lithic wacke
CND1.2	44.3	12.7	0.3	0.0	0.0	2.3	37.0	0.7	2.7	quartz wacke
FON I 00	30.7	7.3	3.3	0.0	1.3	4.0	47.3	1.0	5.0	(sub)arkosic wacke
MON2.8c	51.3	3.3	1.7	0.0	0.7	0.7	40.0	0.7	1.7	quartz wacke
QUI3.1	31.3	2.7	0.3	0.3	1.3	2.7	51.0	0.3	10.0	(sub)lithic wacke
ZOR1.2	31.3	1.0	0.3	0.0	0.3	0.0	60.0	2.7	4.3	quartz wacke

For explanations see Table 3

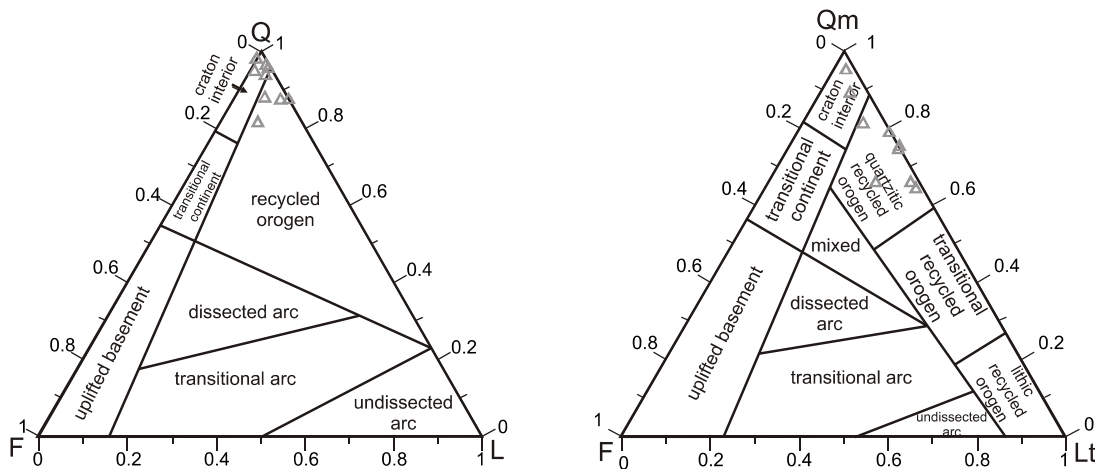


Fig. 4. Ternary QFL (left) and QmFLt (right) plots showing framework modes of the AVU samples

Fields defined by Dickinson *et al.* (1983), for explanations see Table 3

latory quartz varied (10 to 20%) as well as that of polycrystalline quartz (17 to 27%), but in most cases, the latter was more frequent than the former.

Among polycrystalline quartz grains, ones with 3 or more crystal units per grain were clearly dominant (between 73 and 90%), corresponding to chert (*s.l.*) grains and more rarely to very-fine quartzite grains (Fig. 3D).

Apart from the undulosity, there were no relevant petrographic differences between undulose and non-undulose quartz grains. These were characteristically fresh, of variable roundness: from very angular to well-rounded, typically sub-angular or sub-rounded (Fig. 3D, F). Despite the reduced number of samples, all are within the low grade metamorphic field when plotted in the diamond plot of Basu *et al.* (1975). This is in accordance with the composition of the lithoclastic component of the frameworks which was dominated by chert and quartzite grains.

PALYNOLOGY AND PALYNOSTRATIGRAPHY

The organic residue was composed, in most instances, of semi-translucent dark grey to black AOM with subordinate amounts of sporomorphs and organic-walled microplankton. Acritarchs and prasinophytes are commonly present in most samples with ages from Frasnian to early Tournaisian. Phytoclasts are generally rare. The systematic study and significance of the organic-walled microplankton from the AVU will be addressed in a subsequent publication.

The overwhelming majority of the productive samples from the AVU provided poorly preserved sporomorphs. Thus, most of the taxa reported here are left in open nomenclature (see Appendix A). Many of the samples could be assigned to a stage and occasionally to one or to more than one biozones established for the Devonian and the Carboniferous of Western Europe (e.g., Clayton *et al.*, 1977; Strel *et al.*, 1987).

The spore assemblage recovered from the MIN locality (see Fig. 1) of Frasnian age derives from 4 productive samples from which several dozen slides were made. This is one of the few localities that allowed the observation and documentation of palynomorphs using transmitted light.

Spores assignable to the genera *Apiculiretusispora*, *Geminospora*, *Grandispora* and to a lesser extent to *Leio-triletes* and *Retusotriletes* were dominant. Stratigraphically relevant taxa include *Aneurospora* (*Geminospora*) *extensa* morphon (*A. extensa*–*A. goensis*) Turnau, 1999; *Aneurospora* cf. *greggsii* (McGregor) Strel, 1974; *Chelinospora concinna* Allen, 1965; *Contagisporites optivus* var. *vorobjevensis* (Chibrikova) Owens, 1971; *Cristatisporites triangulatus* (Allen) McGregor and Camfield, 1982; cf. *Densosporites devonicus* Richardson, 1960; *Geminospora lemuralata* Balme, 1962 and *Geminospora micromanifesta* (Naumova) Arkhangelskaya, 1985 (see Strel *et al.*, 1987 and Richardson and McGregor, 1986 for known ranges). Two specimens of *Lophozotriletes me dia* Taugourdeau-Lantz, 1967 were found in one of the samples, but not stratigraphically important species such as *Cirratiradites jekhowskyi* Taugourdeau-Lantz, 1967; *Hystricosporites multifurcatus*

(Winslow) Mortimer and Chaloner, 1967; *Pustula tisporites rugulatus* (Taugourdeau-Lantz) Loboziak and Strel, 1981 and *Verrucosisporites bulliferus* Richardson and McGregor, 1986. Furthermore, characteristic species that could be expected to appear together with the described assemblage such as *Ancyrospora* spp., *Emphani sporites* spp. and *Hystricosporites* spp. were not found.

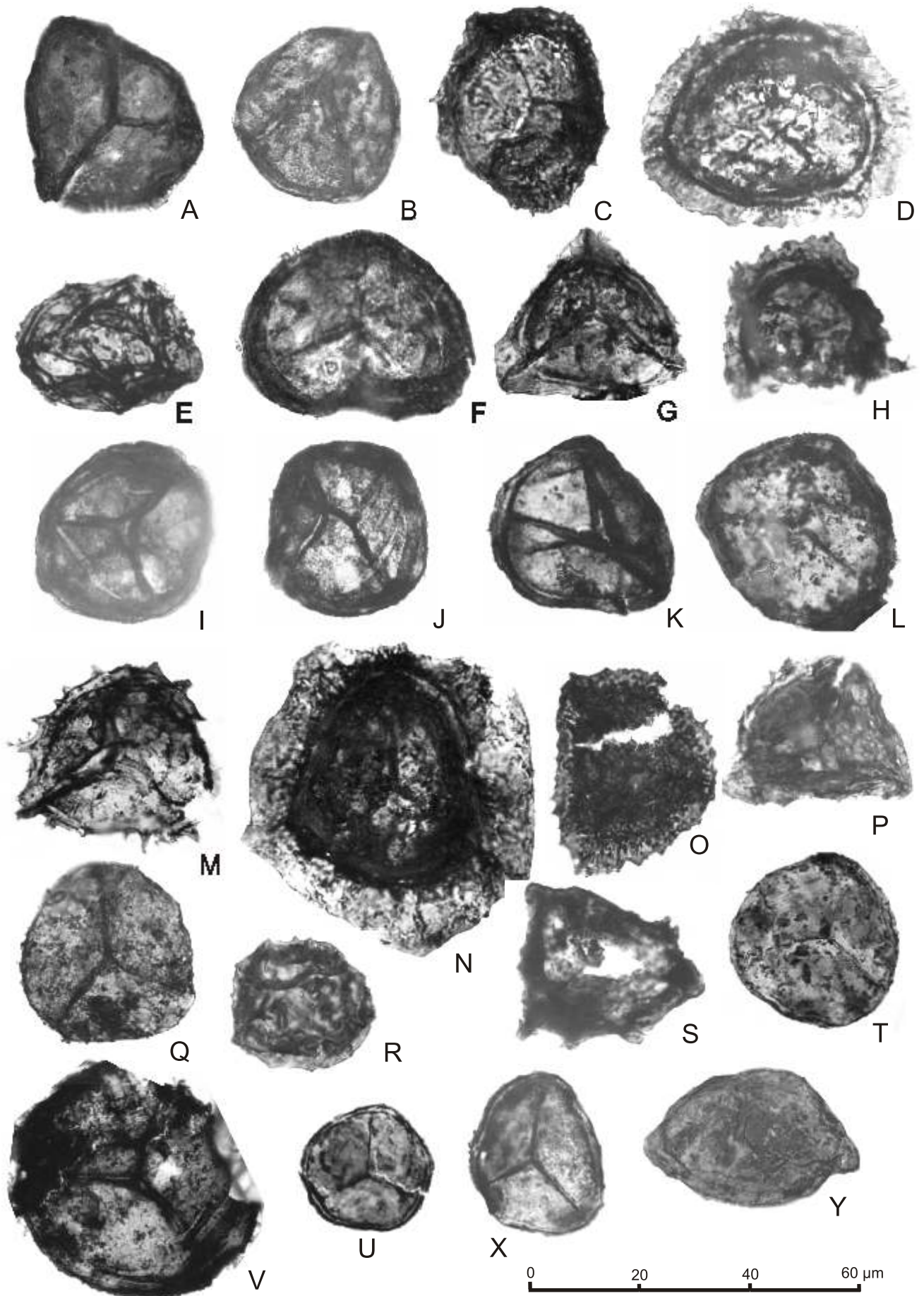
It is worth noting the presence of taxa commonly found in Eastern Europe and Central Asia such as *Geminospora* cf. *aurita* Arkhangelskaya, 1985; *Geminospora micromanifesta* (Naumova) Arkhangelskaya, 1985; *Geminospora notat a* (Naumova) Obukhovskaya, 1993; *Kedoesporis imperfectus* (Naumova) Obukhovskaya and Obukhovskaya, 2008; aff. *Lophotriletes multiformis* Tchibrikova, 1977; *Retusotriletes* cf. *scabratus* Turnau, 1986 (see for example Obukhovskaya *et al.*, 2000; Obukhovskaya and Obukhovskaya, 2008; Fig. 5). The stratigraphic and palaeobiogeographical significance of these taxa is unclear.

Other taxa usually found in older Devonian strata such as *Apiculiretusispora* cf. *perfectae* Steemans, 1989; *Retusotriletes warringtonii* Richardson and Lister, 1969; *Latosporites* cf. *ovalis* Breuer, Al-Ghazi, Al-Ruwaili, Higgs, Steemans and Wellman, 2007 represent a small fraction of the assemblage and are interpreted as reworked (Fig. 5).

Considering the presence of *Chelinospora concinna* Allen, 1965 and *Cristatisporites triangulatus* (Allen) McGregor and Camfield, 1982, this assemblage can be assigned to the *Samarisporites triangulatus*–*Chelinospora concinna* (TCO) miospore biozone of Strel *et al.* (1987), equivalent to the *optivus-triangulatus* miospore biozone of Richardson and McGregor (1986): uppermost Givetian–lowermost Frasnian.

Nearly all other samples produced residues containing palynomorphs not observable by standard transmitted light methods. Documentation of specimens using reflected light microscopy was possible in some cases, but often the resulting images were too blurred to be illustrated. Due to the poor preservation, the standard miospore biozonations of the Devonian and Carboniferous was not directly applicable and stratigraphical palynology was based on the first known occurrence of miospore genera and species.

Famennian and early Tournaisian miospore assemblages are characterized by the presence of *Grandispora* cf. *echinata* Hacquebard, 1957; *Grandispora* aff. *cornuta* Higgs, 1975; *Grandispora* cf. *famenensis* (Naumova) Strel in Becker *et al.*, 1974 var. *minuta* Nekriata, 1974 and especially by *Grandispora gracilis* (Kedo) Strel in Becker *et al.*, 1974 which is present in nearly every sample of this age group and also appears as a reworked form in Viséan samples. Other characteristic taxa are *Corbulispora cancellata* (Waltz) Bharadwaj and Venkatachala, 1961; rarely *Cyrtospora cristifer* (Luber) Van der Zwan, 1979 and *Emphanisporites rotatus* (McGregor) McGregor, 1973; *Rugospora* cf. *flexuosa* (Jushko) Strel in Becker *et al.*, 1974 and *Verrucosisporites nitidus* morphon (*sensu* van der Zwan, 1980; Fig. 7). Late Famennian/early Tournaisian assemblages commonly contain a number of taxa which are probably reworked from (?) Frasnian deposits such as *Hymenozotriletes* spp. and *Archaeoperisaccus* aff. *ovalis* Naumova, 1953 (Fig. 7 and Appendix A).



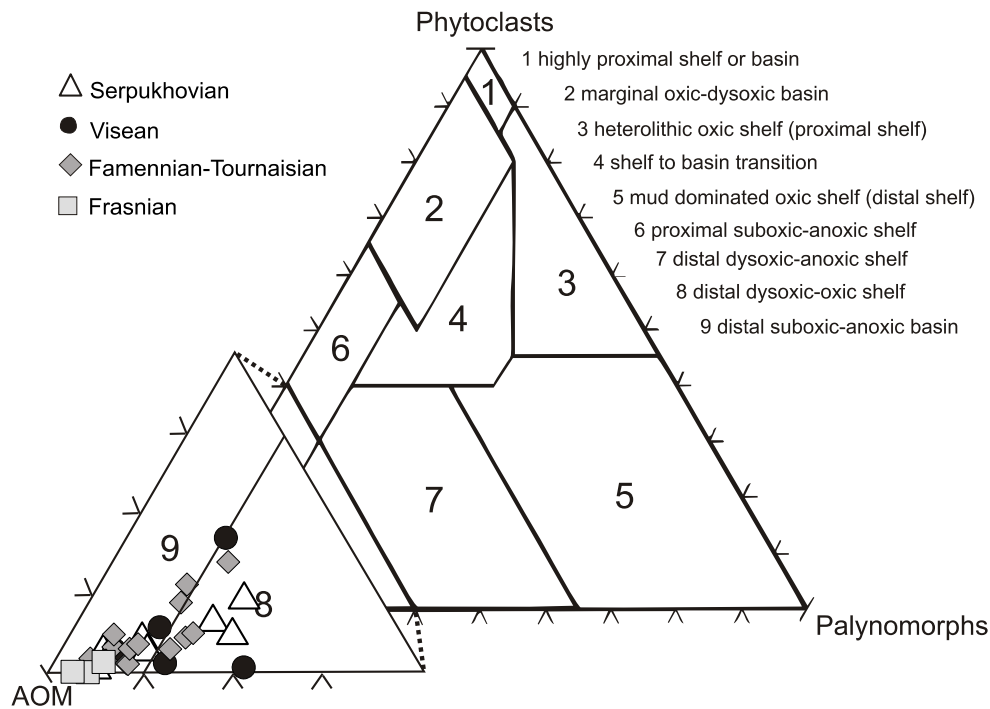


Fig. 6. Ternary Tyson diagram showing the distribution of selected samples from the AVU according to their palynological content (non-sieved slides)

Base diagram adapted from Tyson (1993)

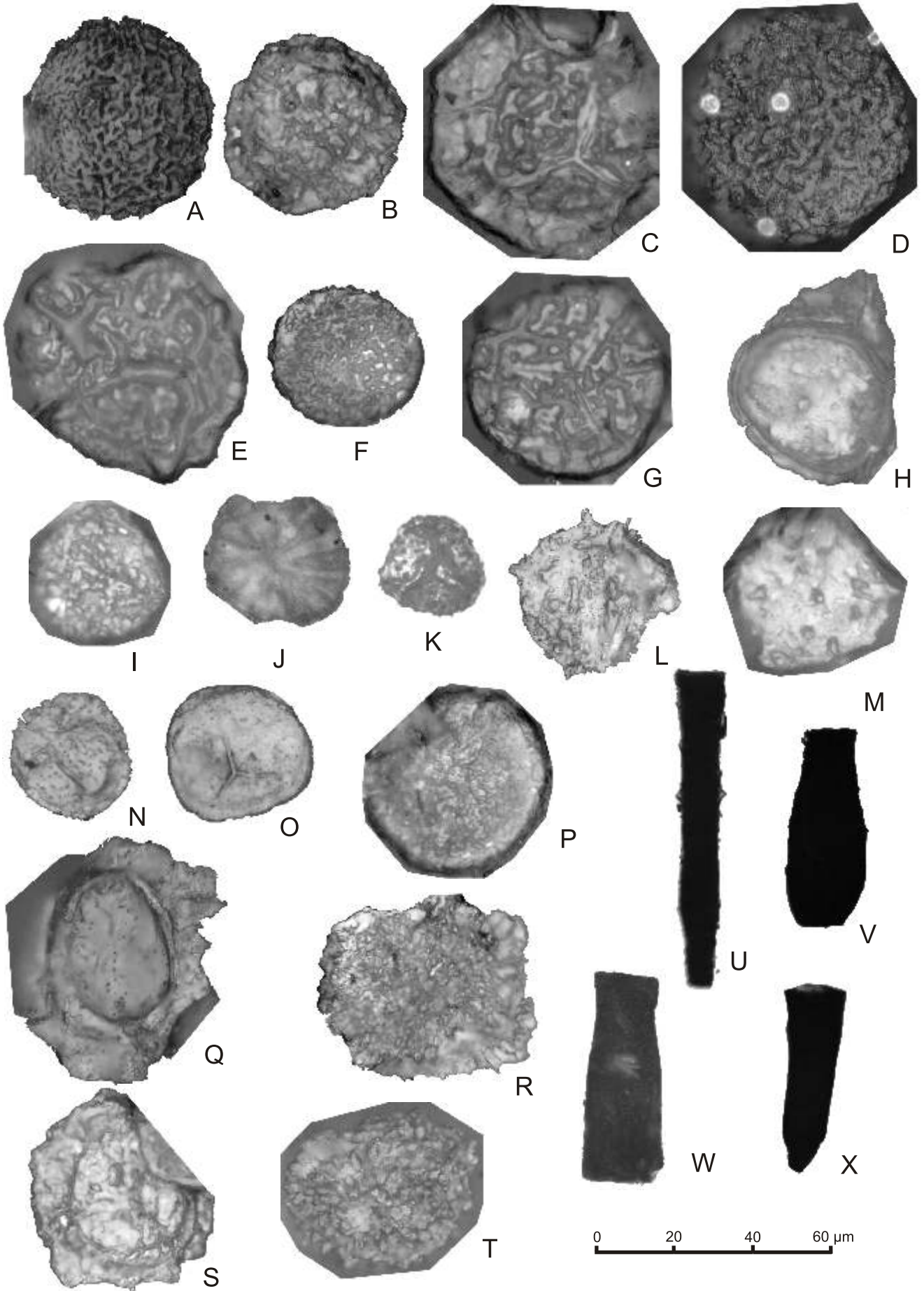
Visean assemblages are difficult to determine but the presence of *Apiculatisporis* cf. *hacquebardi* Playford, 1964; *Densosporites annulatus* (Loose) Smith and Butterworth, 1967; *Lycospora* spp.; *Schulzospora* spp.; *Stenozonotriletes lycosporoides* (Butterworth and Williams) Smith and Butterworth, 1967; *Triquitrites* spp.; *Verrucosporites baccaus* Staplin, 1960 are indicative of this stage (Fig. 8 and Appendix A; see Clayton *et al.*, 1977 for known ranges). It is difficult to match each sample to a specific biozone within the Visean as frequently only one or two characteristic taxa are present.

Serpukhovian assemblages are relatively diverse and several taxa allow the attribution of samples to this stage. Identified taxa include *Acanthotriletes* cf. *aculeolatus* (Kosanke) Potonié and Kremp, 1955; *Apiculatisporis* cf. *variocorneus*

Sullivan, 1964; *Crassispora* aff. *kosankei* (Potonié and Kremp) Smith and Butterworth, 1967; *Dictyotriletes castaneaeformis* (Horst) Sullivan, 1964; *Grumosporites inaequalis* (Butterworth and Williams) Smith and Butterworth, 1967 and other species of this genus; *Leiotriletes* spp.; *Lycospora* cf. *subtriquetra* (Luber) Potonié and Kremp, 1956; *Propriisporites laevigatus* Neves, 1961; cf. *Savitrissporites nux* (Butterworth and Williams) Smith and Butterworth, 1967 (Figs. 8 and 9, Appendix A; see Clayton *et al.*, 1977 for known ranges). It is possible that some samples are actually lower Bashkirian as some of the taxa identified have ranges that extend into the Bashkirian, although none is restricted to this stage. Assemblages assigned to the Serpukhovian usually include several forms which are most likely reworked such as

Fig. 5. Lower (Middle?) Frasnian miospore assemblages

A, B – *Aneurospora* (*Geminospora*) *extensa* morphon (*A. extensa*–*A. goensis*) Turnau, 1999; C – *Aneurospora* cf. *greggsii* (McGregor) Strel, 1974; D – *Auroraspora asperella* variant B (Kedo) Van der Zwan, 1979; E – *Chelinospora concinna* Allen, 1965; F – *Contagisporites optivus* var. *vorobjevensis* (Chibrikova) Owens, 1971; G – *Cristatisporites triangulatus* (Allen) McGregor and Camfield, 1982; H – cf. *Densosporites devonicus* Richardson, 1960; I – *Geminospora* cf. *aurita* Arkhangelskaya, 1985; J – *Geminospora lemurata* Balme, 1962; K – *Geminospora micromanifesta* (Naumova) Arkhangelskaya, 1985; L – *Geminospora notata* (Naumova) Obukhovskaya, 1993; M – *Grandispora tamarae* Loboziak in Higgs *et al.*, 2000; N – *Grandispora* aff. *velata* (Eisenack) McGregor, 1973; O – *Hymenozonotriletes cristatus* Menendez and Pöthe de Baldis, 1967; P – *Kedoesporites imperfectus* (Naumova) Obukhovskaya and Obukhovskaya, 2008; Q – *Leiotriletes* aff. *pagius* Allen, 1965; R – *Lophozonotriletes me dia* Taugourdeau-Lantz, 1967; S – aff. *Lophotriletes multiformis* Tchibrikova, 1977; T – *Retusotriletes* cf. *communis* Naumova, 1953; U – *Retusotriletes minor* Kedo, 1963; reworked; V – *Apiculiretusispora* cf. *perfectae* Steemans, 1989; X – *Retusotriletes warringtonii* Richardson and Lister, 1969; Y – *Latosporites* cf. *ovalis* Breuer, Al-Ghazi, Al-Ruwaili, Higgs, Steemans and Wellman, 2007; all images are transmitted light photomicrographs; all illustrated specimens derive from locality MIN (see Fig. 1)



Apiculatasporites wapsipiniconensis Peppers, 1969; aff. *Geminospora* spp.; *Grandispora* spp.; *Lophozonotriletes* spp.; *Rugospora* spp. and *Samarisporites* sp. (Fig. 9).

PALYNOFACIES

For palynofacies analysis the samples selected were assembled into four age groups for the sake of clarity. The results are graphically represented as several categories and group of categories in ternary plots and bi-dimensional plots with a time axis.

The Tyson diagram (Fig. 6) shows a single sample group plotting near the AOM corner, corresponding to the distal suboxic-anoxic basin and distal dysoxic-oxic shelf fields. There is little differentiation between samples according to their age. Nevertheless there is a poorly defined trend “away” from the AOM corner from older to younger samples. This corresponds to a relative increase in the proportion of palynomorphs (spores and organic-walled microplankton) and to a lesser extent to an increase of phytoclast content.

Frasnian samples plot closely together, very near the AOM corner. Palynomorphs are observable but are statistically irrelevant (Figs. 6 and 9). Phytoclasts are extremely rare. Famennian-Tournaisian samples are concentrated very close to the AOM corner, but extend into the distal dysoxic-oxic shelf field. This is mainly due to the presence of acritarchs and prasinophytes (even though highly fragmented) up to 13% in some samples (Figs. 6 and 9). Spores are also frequent, but never as common as acritarchs and prasinophytes. Visean samples are dispersed, with some plotting very near the AOM corner (AOM around 90%) while others plot within the distal dysoxic-oxic shelf field, corresponding to samples with higher palynomorph or phytoclast content (Figs. 6 and 9). Serpukhovian samples are also dispersed, but can be separated in two groups, one within the distal dysoxic-oxic shelf field, corresponding to samples with higher spore contents (up to 17%) and a second group plotting near the AOM corner – Serpukhovian black shale facies (Figs. 6 and 9). The second group can also be identified in the terrestrial-marine palynomorphs vs. age and spore-organic-walled microplankton vs. age plots (Figs. 10 and 11).

Similarly to the Tyson diagram, the palynofacies analysis of the sieved residues shows some dispersal of data, but some trends are noticeable. The terrestrial-marine palynomorphs vs. age and spore-organic-walled microplankton vs. age plots

(Figs. 10 and 11) show a progressive and irregular increase of terrestrial palynomorphs' content from older to younger samples.

Frasnian samples show some dispersal of data, but both organic-walled microplankton (Fig. 11) and total marine palynomorphs (Fig. 10) are dominant. This reflects the dominance of highly fragmented acritarchs over the spores in the residues. Lithologically, all Frasnian samples correspond to grey shales, often finely laminated. Famennian-Tournaisian samples cover a very wide range in both plots, but most samples show a higher proportion of spores and total terrestrial palynomorphs. This marks the general abundance of spores in the residues of this age. However, some residues were particularly rich in acritarchs and occasionally also in prasinophytes which explains the wide range in both plots. Both types of residues (spore- and acritarch-rich) originated from the black shale lithofacies.

Visean samples are characterized by the abundance of spores in sieved residues. Phytoclasts are more frequent. This is shown in both plots, where single sample groups are observed, around the 90% spore and 75% terrestrial palynomorph axes. Lithologically, Visean samples are grey shales and some highly deformed silty-shales possibly represent turbidites? Serpukhovian samples are divided into two groups, similarly to the Tyson diagram. One shows similar characteristics to the Visean samples, with a high spore content and a generally high content of terrestrial palynomorphs (phytoclasts are relatively frequent). These derive from the sand-silt-shale beds, interpreted as turbidites. The second group has a relatively high content of organic-walled microplankton, few spores and very rare phytoclasts. Organic-walled microplankton is represented by simple polygonomorphs and very small prasinophytes, although identification is difficult as specimens are highly fragmented. Lithologically, these samples are derived from black shales, apparently identical to the Famennian-Tournaisian ones.

ORGANIC GEOCHEMISTRY, SOURCE ROCK POTENTIAL AND ORGANIC MATURITY

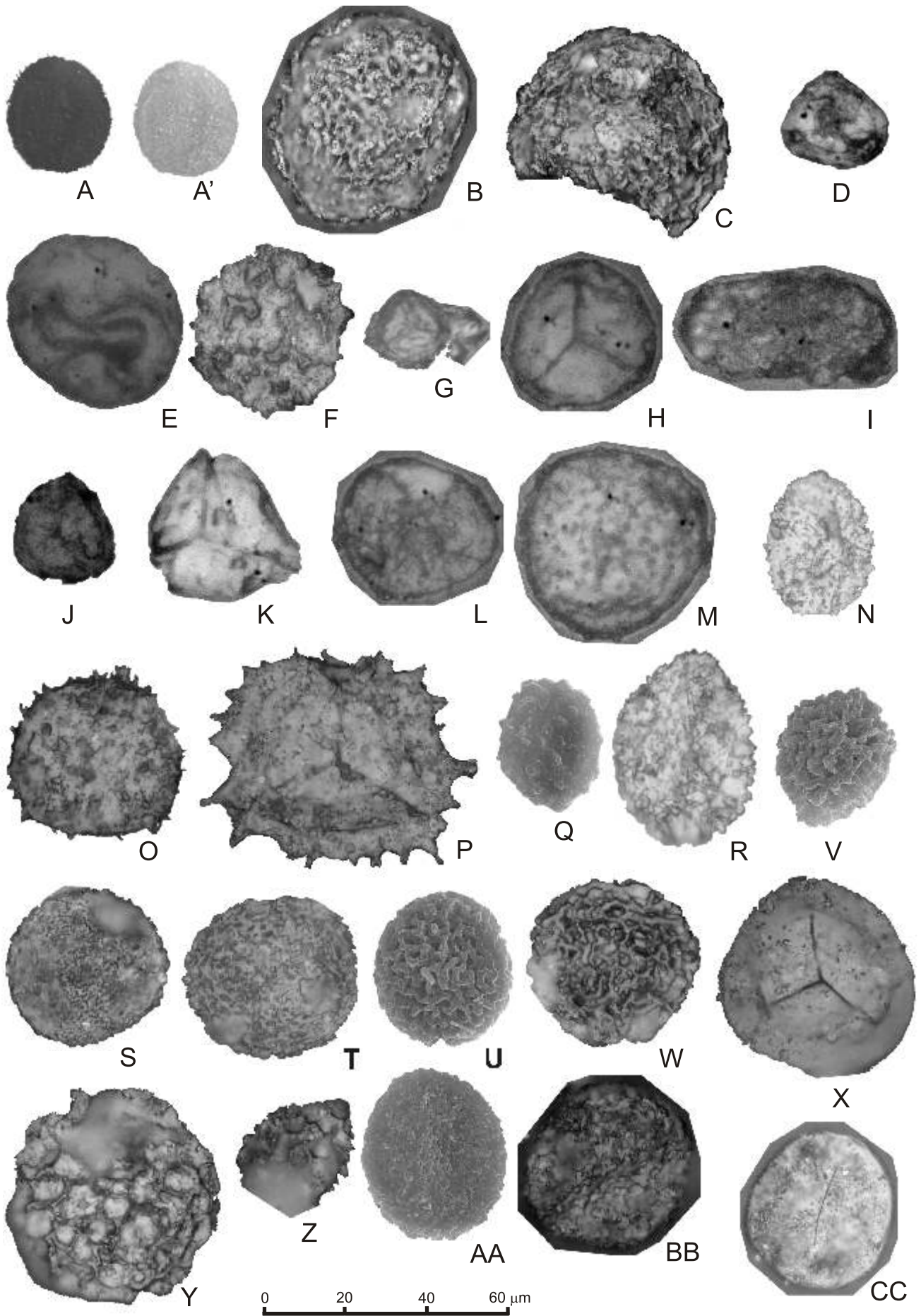
All samples show considerably low TOC values (<0.5 wt.%) and an apparent high maturity. There seems to be little or no differentiation of samples according to their age.

The high maturity is indicated by the low S1 and S2 values (see Fig. 12 and Appendix B). The production index (PI) is also



Fig. 7. Famennian-Tournaisian miospore and chitinozoan assemblages

A – *Convolutispora ce re bra* Butterworth and Williams, 1958 (CAN locality); **B** – *Convolutispora subtilis* Owens, 1971 (VAL locality); **C** – *Convolutispora paraverrucata* McGregor, 1964 (VAL locality); **D** – *Convolutispora varicosa* Butterworth and Williams, 1958 (CAN locality); **E** – *Convolutispora* cf. *vermiformis* Hughes and Playford, 1961 (VAL locality); **F** – *Convolutispora* sp. (VAL locality); **G** – *Corbulispora cancellata* (Waltz) Bharadwaj and Venkatachala, 1961 (VAL locality); **H** – *Cyrtospora cristifer* (Luber) Van der Zwan, 1979 (VAL locality); **I** – *Dictyotriletes submarginatus* (Playford) Van der Zwan, 1980 (VAL locality); **J** – *Emphanisporites rotatus* (McGregor) McGregor, 1973 (BOU locality); **K** – *Grandispora* cf. *echinata* Hacquebard, 1957 (VAL locality); **L** – *Grandispora* aff. *cornuta* Higgs, 1975 (VAL locality); **M** – *Grandispora* cf. *famenensis* (Naumova) Strel in Becker *et al.*, 1974 var. *minuta* Nekriata, 1974 (VAL locality); **N** – *Grandispora gracilis* (Kedo) Strel in Becker *et al.*, 1974 (VAL locality); **O** – *Punctatisporites minutus* Kosanke, 1950 (VAL locality); **P** – *Rugospora* cf. *flexuosa* (Jushko) Strel in Becker *et al.*, 1974 (VAL locality); reworked; **Q** – *Archaeoperisaccus* aff. *ovalis* Naumova, 1953 (TAP locality); **R–T** – *Hymenozonotriletes* spp. (R and S – VAL locality, T – TAP locality); **U–X** – Chitinozoan (V and X – VAL locality, U and W – ASS locality); all images are reflected light photomicrographs, except K, U, V, W and X which are transmitted light microphotographs



very low (<0.6) and indicates high thermal maturity equivalent to the dry gas generation zone. This is consistent with the observed maturity seen in palynological slides. The vast majority of the organic residues analysed have slightly translucent to opaque, black spores, indicating a thermal alteration index (TAI) > 4+.

Under a reflected light microscope, very few particles could be positively identified as vitrinite, since petrological information is lost in palynological residues. Nevertheless, all particles measured indicate reflectance values higher than 3%.

The T_{max} values below 400°C do not represent kerogen maturity and are related to residual bitumen or exsudatinitite.

The AVU samples have considerably low values of hydrogen index (HI; <60 mgHC/g TOC) and oxygen index (OI; <190 mgCO₂/g TOC), thus most of them plot in the area where the 3 types of kerogen line merge, providing no indication on kerogen types (Fig. 13 and Appendix B). However, 3 samples (MIN16.3, MIR4.3 and ALH1.4) plot within the kerogen type III field, i.e., gas-prone and usually associated with terrestrially-derived organic matter. The palynofacies data indicate that terrestrial influence was slight, even for the more proximal environments recorded in some rocks of Serpukhovian age. The organic residues of the AVU are typically marine AOM-rich (>85% of total organic residue) with accessory amounts of organic-walled microplankton, spores and generally rare or very rare phytoclasts.

The source rock potential of the samples analysed seems limited. This is readily indicated by the low TOC values (<0.5 wt.%) and also by the low S1 and S2 values (≤0.05 mgHC/g rock). The palynofacies analysis of shale samples of the AVU invariably indicates oil-prone source rocks, although this method does not give an estimate of the proportion of the hydrocarbon-prone material per weight or volume of rock.

DISCUSSION

The observed sand/mud ratio at the outcrop scale varies greatly, but, with few exceptions, mud clearly dominates and the sand is usually medium to fine. Most of the relatively

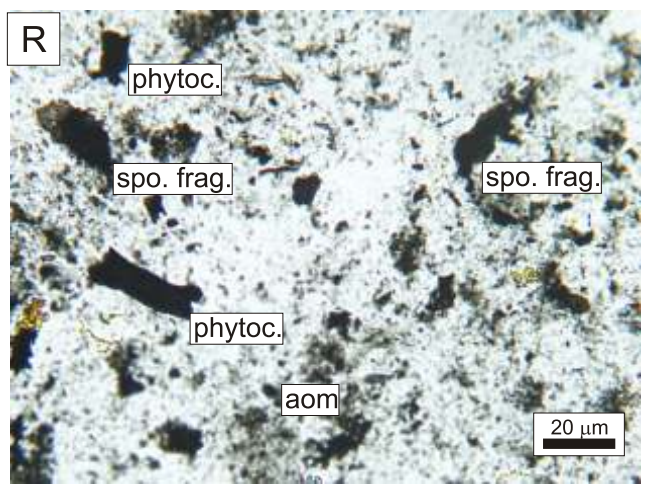
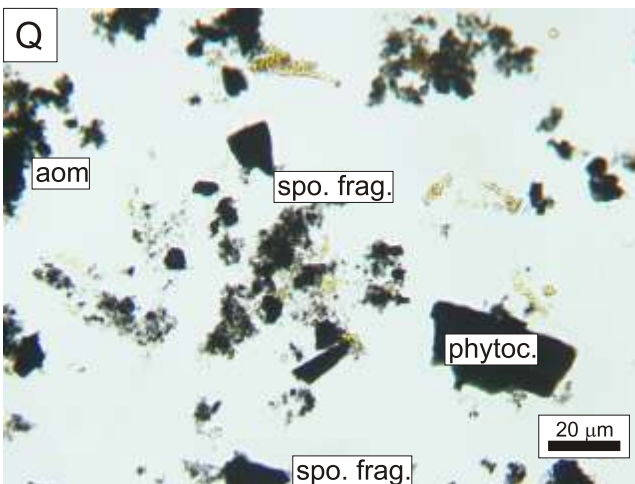
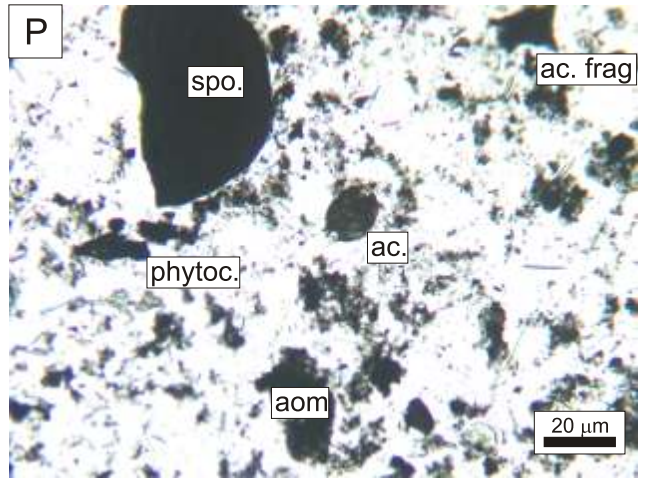
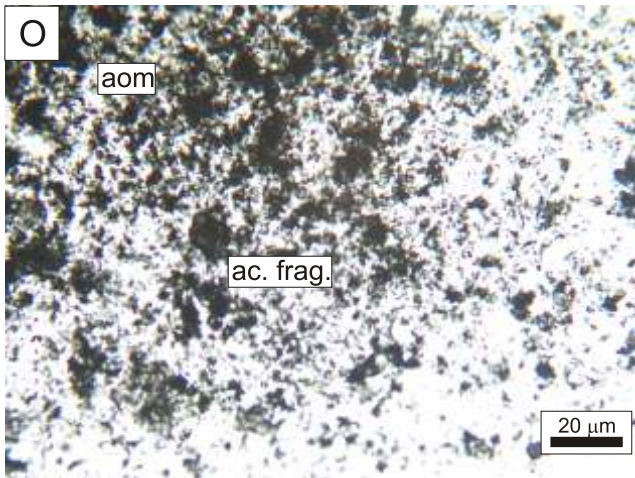
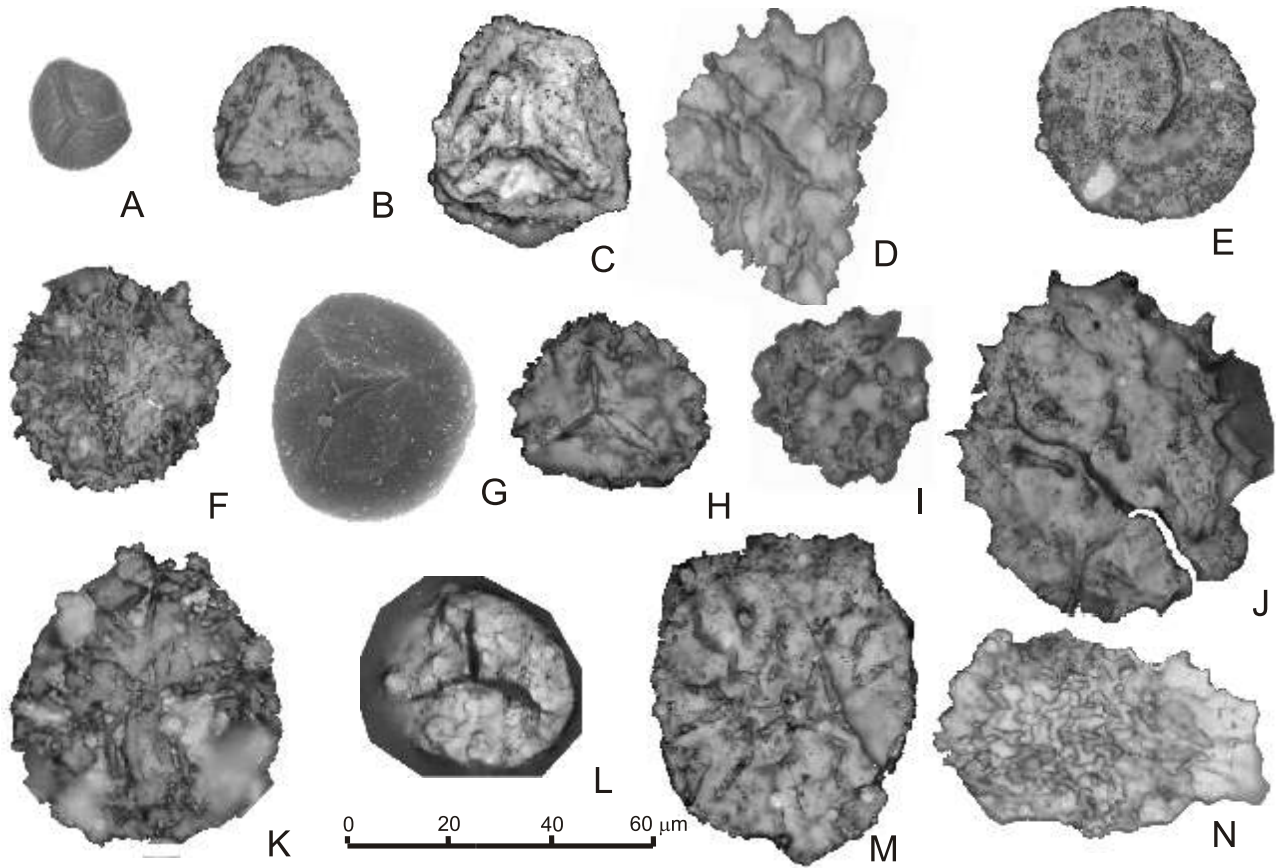
undeformed sections (sand-silt-shale facies) show a turbiditic character. The textural maturity of the sandstones and the general dominance of mud over sand imply the existence of a large and essentially low relief drainage area and also the presence of a deltaic system (or coastal plain?) where most of the coarser sediments were trapped (Bouma, 2000a, b; see Fig. 14). A similar sedimentary setting, associated with a large deltaic system, was described by Ahrens (1936) and Stets and Schäfer (2008) from the Central Facies Belt of the Devonian of the Rheohercynian basin. Although deformed and slightly metamorphosed in some areas, the gradual passage from deltaic subaerial (to the NW) to shallow marine and to deeper marine settings (to the SE) is clearly observed in this basin. In the case of the AVU, it is possible that only the distal parts of such a sedimentary system were preserved.

The newly collected sedimentary information from the Serpukhovian sections strongly suggests that a turbidite system close to the fine-grained end member (*sensu* Bouma, 2000a, b) is represented by the metasedimentary rocks of the AVU of this age. The observed turbidite sequences can be generally included in facies association V and more rarely IV (BOS section) of Mutti and Normark (1987), indicating distal (rarely intermediate) lobe depositional elements. The sedimentary packages composed essentially or entirely of shales (black shale and laminated grey shale facies) within this unit are volumetrically important and are not always associated (at least spatially) with packages identified as turbidites. These shale packages may represent the distal parts of lobes formed by turbidite deposition and/or hemipelagic deposits.

The dominance of quartz (and quartzose clasts – cherts and quartzites) in the sandstones imply that the detrital framework modes (Serpukhovian sections) described here derive from detritus with a significant compositional maturity (e.g., Prothero and Schwab, 1996), although the high proportion of matrix/cement indicates a low textural maturity (*sensu* Folk, 1951). This textural characteristic may have been substantially altered by the very low grade metamorphism to which this unit was exposed. Such changes in the matrix nature are observable in some of the samples (Fig. 3F). In addition the textural characteristics may be related to the type of sediment reaching the

Fig. 8. Visean and Serpukhovian miospore assemblages

Visean miospore assemblages: **A**, **A'** – *Apiculatisporis* cf. *hacquebardi* Playford, 1964 (PIC locality); **B** – *Convolutispora* cf. *ce re br* Butterworth and Williams, 1958 (FRA locality); **C** – *Convolutispora* sp. (FRA locality); **D** – cf. *Densosporites annulatus* (Loose) Smith and Butterworth, 1967 (FRA locality); **E** – *Knoxisporites* sp. (TOR locality); **F** – *Lophozonotriletes* sp. (FRA locality); **G** – *Lycospora* sp. (FRA locality); **H** – *Retusotriletes incohatus* Sullivan, 1964 (CAT locality); **I** – *Schulzospora* sp. (CHE locality); **J** – *Stenozonotriletes lycosporoides* (Butterworth and Williams) Smith and Butterworth, 1967 (TOR locality); **K** – *Triquitrites* sp. (PIC locality); **L** – *Verrucosisporites baccatus* Staplin, 1960 (CAT locality); reworked: **M** – *Grandispora* cf. *gracilis* (Kedo) Strel in Becker *et al.*, 1974 (CAT locality); Serpukhovian miospore assemblages: **N** – *Acanthotriletes* cf. *aculeolatus* (Kosanke) Potonié and Kremp, 1955 (FON locality); **O** – *Acanthotriletes* aff. *echinatus* Hoffmeister, Staplin and Malloy, 1955 (AM11 locality); **P** – cf. *Ancyrospora? andevalensis* González, Playford and Moreno, 2005 (AM11 locality); **Q** – *Apiculatisporis* cf. *porosus* Williams in Neves *et al.*, 1973 (SER locality); **R** – *Apiculatisporis* cf. *variocorneus* Sullivan, 1964 (FON locality); **S** – *Convolutispora* cf. *ampla* Hoffmeister, Staplin and Malloy, 1955 (AM11 locality); **T** – *Convolutispora ce re br* Butterworth and Williams, 1958 (AM11 locality); **U** – *Convolutispora circumvallata* Clayton, 1971 (SER locality); **V** – *Convolutispora* aff. *disparalis* Allen, 1965 (SER locality); **W** – *Convolutispora subtilis* Owens, 1971 (FON locality); **X** – *Densosporites annulatus* (Loose) Smith and Butterworth, 1967 (AM11 locality); **Y** – *Dictyotriletes* cf. *aequalis* Staplin, 1960 (AM11 locality); **Z** – *Dictyotriletes castanaeformis* (Horst) Sullivan, 1964 (FON locality); **AA** – *Grumosisorites inaequalis* (Butterworth and Williams) Smith and Butterworth, 1967 (SER locality); **BB** – *Grumosisorites* sp. (FON locality); **CC** – *Laevigatosporites* spp. (MON locality); all are reflected light photomicrographs except: **A** and **A'** which are transmitted light photomicrographs; **Q**, **V**, **U**, **AA** which are SEM photomicrographs



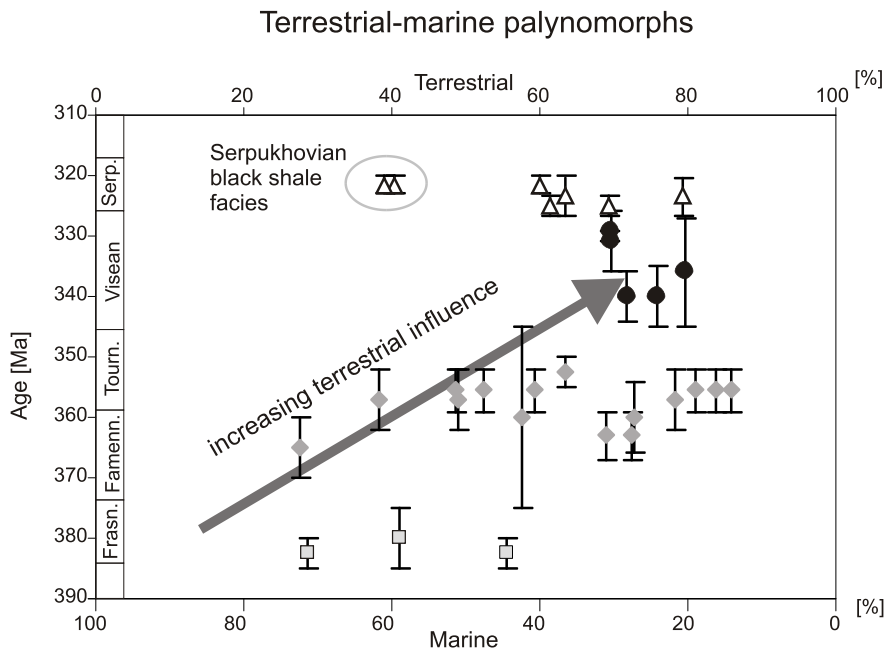


Fig. 10. Terrestrial-marine palynomorphs vs. age

Plot of selected 7 µm-sieved residues from the AVU; see Table 2 for the grouping of categories; error bars on Y-axis based on the uncertainty of the biostratigraphical determination of each sample; ages compiled from *Time Scale Creator* software (Gradstein *et al.*, 2004); for other explanations see Figure 6

shelf areas (which was very likely mud-rich) and later transported by turbidity currents (Fig. 14).

The original data-set used by Dickinson and Suczek (1979) for sediment provenance analysis included only samples with matrix/cement proportion less than 25%, which can limit the significance of the collected data.

The distribution of the detrital framework data-set within the craton interior and quartzitic recycled orogen fields may reflect a drainage basin located on an essentially stable cratonic area (CIZ?) which may have a collisional or transcurrent character along its margin. The results from the undulosity of quartz, although restricted to a few samples, clearly indicate that the sediments of the AVU derived from rocks of low metamorphic grade. This is consistent with the observed presence of quartzite and chert grains. The CIZ is a potential sediment source area (see Fig. 14). This zone is at

present adjacent to the AVU and composed essentially of low grade metasedimentary rocks of late Proterozoic–Cambrian age (Carrington da Costa, 1950; Medina *et al.*, 1989, 1993) overlain by Ordovician (namely the Armoricain quartzite very near the CIZ boundary) to Lower Devonian very low grade metasedimentary rocks (e.g., Cooper, 1980; Paris, 1981; Oliveira *et al.*, 1992; Fig. 9). The timing of the metamorphic event (or events) that affected the CIZ and the time at which these rocks were exposed and eroded is certainly pre-late Pennsylvanian as indicated by the presence of CIZ-derived clasts in the sediments of the Buçaco Basin (Gama Pereira, 1987; Machado, 2010). It is uncertain, however, if they were already exposed by Late Devonian times. It has been suggested (Chaminé *et al.*, 2003b) that the PTSZ was already active during the Late Devonian and Mississippian, controlling the regional sedimentation by forming scattered pull-apart like and/or fault-wedge basins in a marine setting near a continental block. The results presented here suggest that such tectonic activity may have been affecting the continental block where the source areas were located, but probably did not affect the shelf and basin floor where sedimentation was occurring (Fig. 14). Neither intraclasts nor lithoclasts from the closely associated Arada Unit were found in the frameworks analysed. These would be expected if significant tectonic activity (and consequent recycling) was occurring within the sedimentation area (compare for example McCann, 1991; Burnett and Quirk, 2001).

The palynofacies analysis presented here, coupled with the lithological and sedimentological characteristics of the metasedimentary rocks of the AVU show some palaeo-environmental variations through time. A single sedimentation environment (*s.s.*) seems to be recorded from Frasnian deposits (laminated grey shales). A marine, most likely basinal setting is indicated by the finely laminated shales with a typical marine

Fig. 9. Serpukhovian miospore assemblage and examples of unsieved organic residues

A – *Leiotriletes ornatus* Ischenko, 1956 (SER locality); B – *Leiotriletes* sp. (AM11 locality); C – *Lycospora* cf. *subtriquetra* (Luber) Potonié and Kremp, 1956 (AM11 locality); D – *Proprisporites laevigatus* Neves, 1961 (FON locality); E – *Punctatisporites irrasus* Hacquebard, 1957 (AM11 locality); F – aff. *Radialeles* sp. (AM11 locality); G – *Retusotriletes* sp. (SER locality); H – cf. *Savitrissporites nux* (Butterworth and Williams) Smith and Butterworth, 1967 (AM11 locality); I – *Verrucosissporites* cf. *scurrus* (Naumova) McGregor and Camfield, 1982 (AM11 locality); reworked: J – *Grandispora* aff. *tamarae* Loboziak in Higgs *et al.*, 2000 (AM11 locality); K – *Emphanisporites* sp. (FON locality); L – *Lophozonotriletes* sp. (AM11 locality); M – *Rugospora* cf. *flexuosa* (Jushko) Streel in Becker *et al.*, 1974 (AM11 locality); N – *Samarisporites* sp. (FON locality); unsieved organic residues: O – example of a Frasnian non-sieved residue (RET locality); P – example of a Famennian non-sieved residue (VAL locality); Q – example of a Visean non-sieved residue (FRA locality); R – example of a Serpukhovian non-sieved residue (FON locality); ac. – acritarch (*s.l.*), aom – amorphous organic matter, frag. – fragment, phytoc. – phytoclast, spo. – spore; all are reflected light photomicrographs except: A, O, P, Q, R which are transmitted light photomicrographs; G which is a SEM photomicrograph

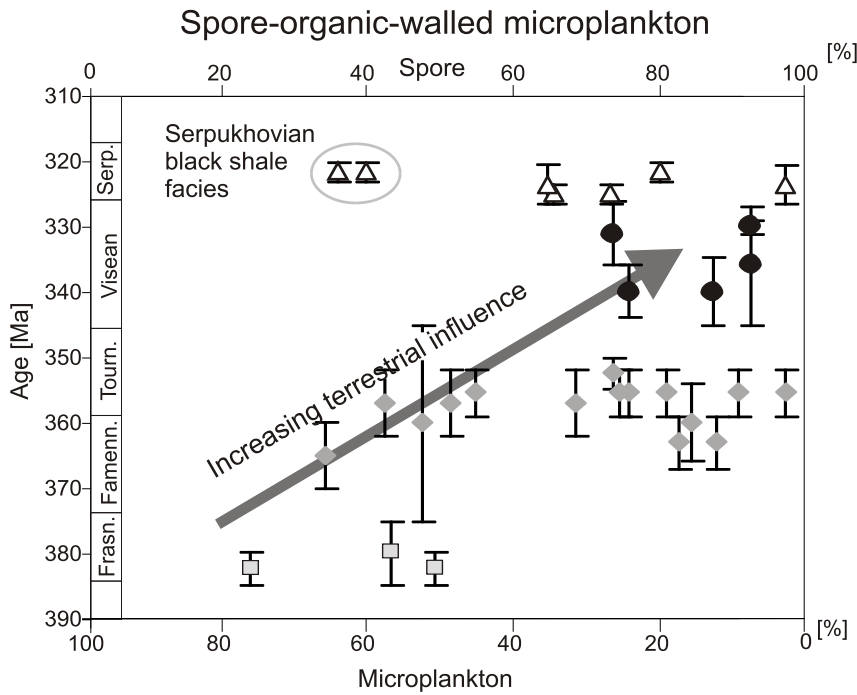


Fig. 11. Spore-organic-walled microplankton (acritarch and prasinophytes) vs. age

For other explanations see [Figures 4 and 5](#)

palynological association. The constant presence of organic matter and significant proportion of AOM, shown by palynological analysis, along with the cm- to mm-lamination and the absence of bioturbation implies that, generally, the marine organic productivity in the water column was high, but also that the oxygen minimum zone was near or below the sediment-water interface where sedimentation was taking place (e.g., Curtis, 1980; Calvert, 1987). A similar environment with laminated sediments

when compared with Frasnian samples, indicated by the greater presence of spores and slightly higher phytoclast content.

The Viséan and Serpukhovian strata are generally coarse-grained, with the appearance of turbidite and (?)pro-delta deposits, but the black shale and laminated grey shale facies persist, indicating a diversity of sedimentary environments. The amount of terrestrial input is higher, indicated by the generally coarse-grained sediments but also the greater

forming in areas where the oxygen minimum intersected the ocean floor has been described, for example, by Calvert (1964) and Donegan and Schrader (1982) in the Gulf of Mexico. The characteristics of the palynological content of Frasnian samples are in accordance with this interpretation. The lighter and darker laminae commonly found can be described as rhythmites. The origin and processes responsible for this rhythmical sedimentation are difficult to determine. A distal deltaic suspension fall out sedimentation type with a seasonal control can perhaps explain the observed sedimentary features. This lithofacies is also observed in the Viséan and Serpukhovian (more rarely in Famennian–Tournaisian) rocks and, presumably, the sedimentary environment where these facies developed prevailed through time.

The Famennian and Tournaisian rocks are, in most instances, black shales, with a characteristic palynological content; AOM-rich along with a diverse organic-walled microplankton assemblage. The terrestrial influence is increased,

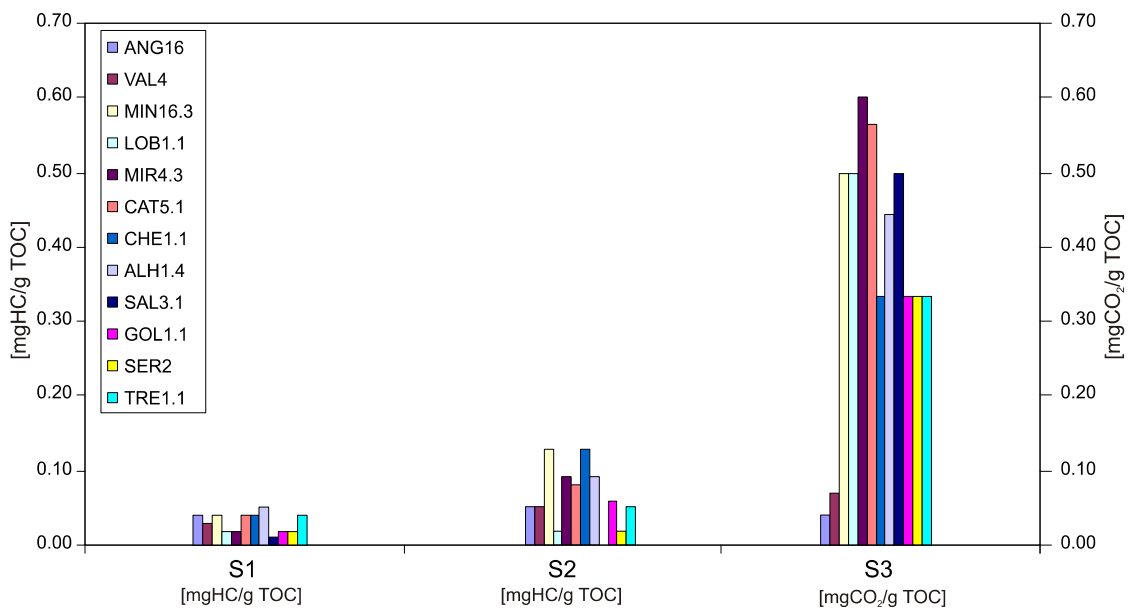


Fig. 12. S1, S2 and S3 values for the samples analysed from the AVU

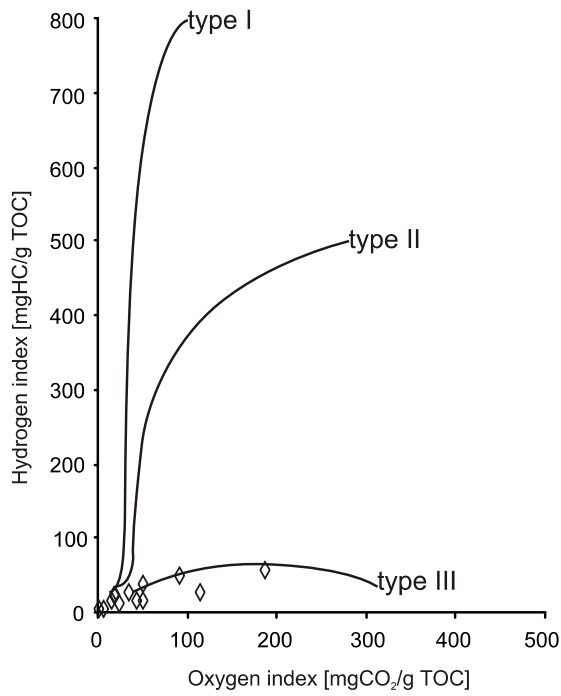


Fig. 13. Van Krevelen diagram with 3 main types of kerogen and the HI/OI ratios of the AVU samples

Original diagram from Tissot and Welte (1984)

amount of spores and, to a lesser extent, the greater amount of phytoclasts. AOM proportions decrease slightly. It should be mentioned that acritarch diversity and abundance decreases globally in the latest Devonian and especially during the Mississippian (see Strother, 2008 and Riegel, 2008 for a revision of previous work and causes) which could have influenced the results obtained from palynofacies analyses. Nevertheless, other palynological and lithological indicators point to the same conclusions.

The thermal and burial history of the AVU as a whole started after the Serpukhovian (youngest) deposits and lasted, in a first phase, to the Early Triassic. This is indicated by the outcrop-scale observation of Lower Triassic strata of the Lusitanian Basin (Grés de Silves Fm.) resting unconformably over the AVU at several localities and also by the associated ferruginization of the AVU in these areas (see Fig. 3A). The intramontane Gzhelian Buçaco Basin (Wagner *et al.*, 1983; Pinto de Jesus *et al.*, 2010; Flores *et al.*, 2010; Machado, 2010 and references therein) does not rest unconformably over the AVU – the contacts are invariably fault-bounded (Gama Pereira *et al.*, 2008; Flores *et al.*, 2010).

The basin represented by the AVU most probably extended far beyond the influence of the PTSZ and may be preserved as basement under the Lusitanian Basin, both on- and off-shore (see Bless *et al.*, 1977; Capdevila and Mougenot, 1988; Moço *et al.*, 2001). Indeed, samples from shallow boreholes in the Lusitanian Basin (Estarreja and Ovar area) that reached the basement indicate the presence of shales of similar

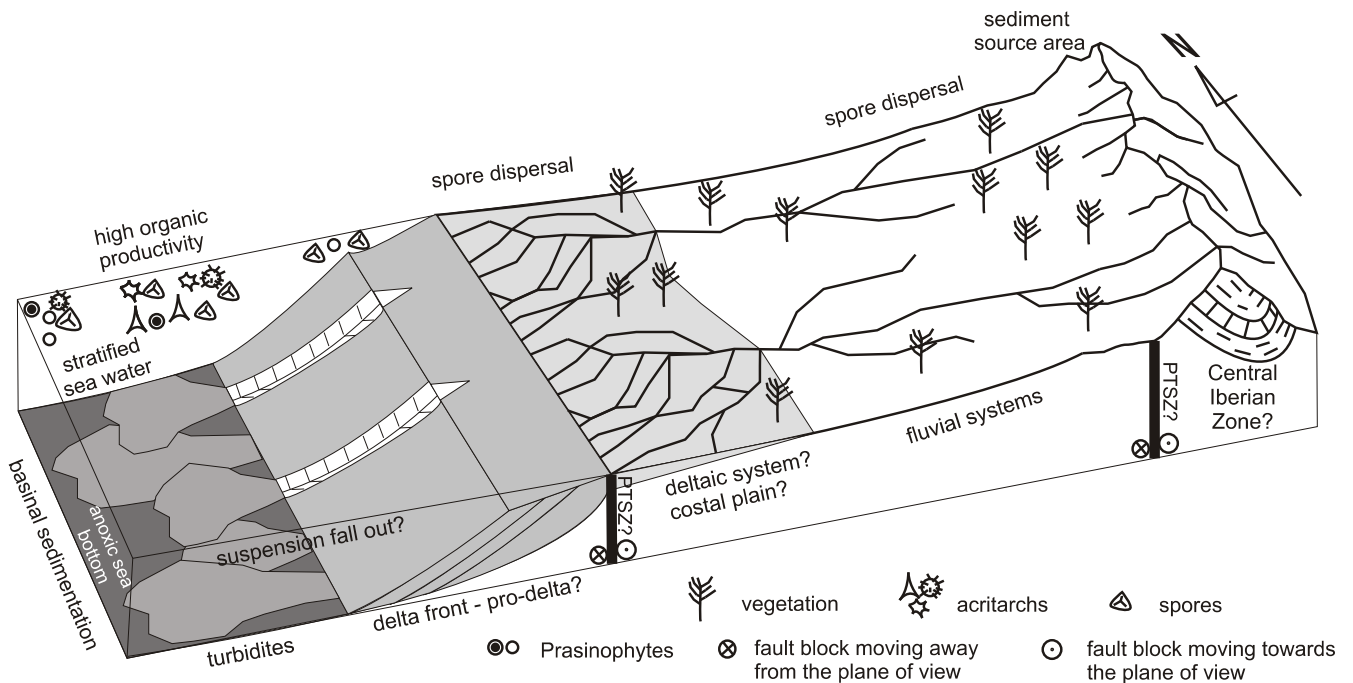


Fig. 14. General schematic and non-age specific representation of the hypothetical tectonic and sedimentation setting (km- to 100 m-scale) of the AVU

No vertical scale implied

palynological content (regarding age and palynofacies) to the AVU (ACC01, ACC15, AC52 wells in Fig. 1).

It is worth noting the possible significance of the AVU as a shale gas source rock. It is within the dry gas generation zone; it is volumetrically quite important both at the surface and subsurface (although its true volume and extension are still unknown) and it is highly fractured. It is uncertain if the low TOC values present here are representative of the AVU preserved in the subsurface. The van Krevelen diagram points to a gas-prone rock which is in contrast with the palynological content of this unit (which clearly indicates an oil-prone source). This can be explained by the current thermal maturity of the AVU – dry gas generation zone – which would result in the observed OI/HI ratios.

CONCLUSIONS

The new palynological data presented here indicate that the deposition of the AVU happened between the (?)early Frasnian and the Serpukhovian. This is coherent with the preliminary results of Fernandes *et al.* (2001). The new data allowed a refinement of the known ages for the AVU and the identification of characteristic lithofacies over several time intervals.

The sedimentological data collected implies that the post-sedimentary tectonic evolution of the area, clearly associated with the partition of the crustal deformation along the PTSZ (Chaminé *et al.*, 2003a, b, 2007), destroyed most of the sedimentary record and preserved only a few discrete portions (AVU) of a much larger basin (see Fig. 14). The sediment source areas were most probably located in the CIZ (Proterozoic and Paleozoic metasedimentary rocks).

Overall it seems the sedimentary system has a general prograding tendency, from basinal distal deposits during the Frasnian to more proximal settings in the Viséan and especially during the Serpukhovian where sand- and silt-dominated

turbidites seem to have prevailed (Fig. 14). The palynofacies results are consistent with the sedimentological results, with an increasing terrestrial influence – spores and phytoclasts become more common, AOM and organic-walled microplankton decrease proportionally – from older to younger deposits.

The AVU maturation data and regional geology indicate that the exhumation of the AVU happened between the late Pennsylvanian and the Late Triassic. They also show that the thermal and generally the geological history of the basin represented by the AVU in this region were significantly controlled by the PTSZ which was tectonically active at least from the late Pennsylvanian.

The potential hydrocarbon play system formed by the AVU, Buçaco Basin deposits and the Lusitanian Basin lacks the correct timing of events within and near the PTSZ. Its potential may be greater as shale gas play in regions outside the influence of this shear zone.

Acknowledgements. Á. Pinto and R. Jorge from Creminer (Faculdade de Ciências da Universidade de Lisboa) and M. Cachão from Centro de Geologia-FCUL for the logistical support; A. Verde (FCUL) for support with the thin sections. E. Soares and L. Carvalho from Aveiro University are acknowledged for their technical support with the microwave digestion system. Thanks are also due to J. P. Fernandes, L. P. Moço, A. Pinto de Jesus, M. J. Lemos de Sousa and A. A. Soares de Andrade for all discussions in early stages of the research. Funding for part of this research was provided by the Fundação para a Ciência e a Tecnologia PhD grant SFRH/BD/23787/2005 (G. Machado). This work was performed under the framework of the PEst-C/CTE/UI4035/2011 (Projecto Estratégico - UI 4035 - 2011/2012) from the GeoBioTec|UACentre. We acknowledge the two referees for the constructive reviews that helped to improve the clarity of the manuscript.

REFERENCES

- AHRENS W. (1936) – Erläuterungen zur geologischen Karte v. Pressen u. benachbarten dt. Ländern, Blatten Mayen, Berlin. 47S.
- BATTEN D. J. (1996a) – Chapter 26A. Palynofacies and palaeoenvironmental interpretation. In: Palynology: Principles and Applications (eds. J. Jansonius and D. C. McGregor). Am. Ass. Strat. Palynol. Found., **3**: 1011–1064.
- BATTEN D. J. (1996b) – Chapter 26B. Palynofacies and petroleum potential. In: Palynology: Principles and Applications (eds. J. Jansonius and D. C. McGregor). Am. Ass. Strat. Palynol. Found., **3**: 1065–1084.
- BASU A., YOUNG S. W., SUTTNER L. J., JAMES W. C. and MACK G. H. (1975) – Re-evaluation of the use of undulatory extinction and polycrystallinity in detrital quartz for provenance interpretation. J. Sediment. Res., **45** (4): 873–882.
- BEETSMA J. J. (1995) – The late Proterozoic/Paleozoic and Hercynian crustal evolution of the Iberian Massif, N Portugal, as traced by geochemistry and Sr-Nd-Pb isotope systematics of pre-Hercynian terrigenous sediments and Hercynian granitoids. Vrije Universiteit Amsterdam. Unpubl. PhD Thesis.
- BLESS M. J., KIMPE W. F., MEESSEN J. P., BOUCKAERT J., DEJONGHE L., GRAULICH J. M., CALVER M. A., PAPROTH E., HORN M., KULLMANN J., OLIVEIRA J. T., PARIS F., ROBARDET M., PERDIGÃO J. C., RIBEIRO A., SANCHEZ De POSADA L., TRUYOLS J. and NAYLOR D. (1977) – Y a-t-il des hydrocarbures dans le pre-Permien de l'Europe occidentale? Ministère Affaires Economiques (Services Géologiques), Bruxelles. Prof. Pap., **148** (11): 18–54.
- BOUMA A. H. (1962) – Sedimentology of some flysch deposits: a graphic approach to facies interpretation. Elsevier.
- BOUMA A. H. (2000a) – Coarse-grained and fine-grained turbidite systems as end member models: applicability and dangers. Mar. Petrol. Geol., **17**: 137–143.
- BOUMA A. H. (2000b) – Fine-grained, mud-rich turbidite systems: model and comparison with coarse-grained, sand-rich systems. In: Fine-grained Turbidite Systems (eds. A. H. Bouma and G. C. Stone). Am. Ass. Petrol. Geol. Mem., 72/SEPM Spec. Publ., **68**: 9–20.

- BURNETT D. J. and QUIRK D. G. (2001) – Turbidite provenance in the Lower Palaeozoic Manx Group, Isle of Man: implications for the tectonic setting of Eastern Avalonia. *J. Geol. Soc.*, **158** (6): 913–924.
- CALVERT S. E. (1964) – Factors affecting distribution of laminated diatomaceous sediments in the Gulf of California. In: *Marine Geology of the Gulf of California* (eds. T. H. van Andel and G. G. Shor). *Am. Ass. Petrol. Geol. Mem.*, **3**: 311–330.
- CALVERT S. E. (1987) – Oceanographic controls on the accumulation of organic matter in marine sediments. *Geol. Soc. London, Spec. Publ.*, **26** (1): 137–151.
- CAPDEVILA R. and MOUGENOT D. (1988) – Pre-Mesozoic basement of the western Iberian continental margin and its place in the Variscan Belt (eds. G. Boillot and E. L. Winterer). *Proc. of the Ocean Drilling Program, Sc. Res.*, **103**: 3–12.
- CARRINGTON da COSTA J. (1950) – Notícia sobre uma carta geológica do Buçaco, de Nery Delgado. *Serv. Geol., Portugal*.
- CHAMINÉ H. I. (2000) – Estratigrafia e estrutura da faixa metamórfica de Espinho-Albergaria-a-Velha (Zona de Ossa-Morena): implicações geodinâmicas. Universidade do Porto. Unpubl. PhD Thesis.
- CHAMINÉ H. I., FONSECA P. E., PINTO de JESUS A., GAMA PEREIRA L. C., FERNANDES J. P., FLORES D., MOÇO L. P., CASTRO R. D., GOMES A., TEIXEIRA J., ARAÚJO M. A., SOARES de ANDRADE A. A., GOMES C. and ROCHA F. (2007) – Tectonostratigraphic imbrications along strike-slip major shear zones: an example from the early Carboniferous of SW European Variscides (Ossa-Morena Zone, Portugal). In: *Proc. XVth Internat. Congress on Carboniferous and Permian Stratigraphy* (Utrecht, 2003) (ed. T. Wong): 405–416. Royal Dutch Academy of Arts and Sciences, Amsterdam, Edita NKAW.
- CHAMINÉ H. I., FONSECA P. E., ROCHA F., MOÇO L. P., FERNANDES J. P., GAMA PEREIRA L. C., GOMES C., LEMOS de SOUSA M. J. and RIBEIRO A. (2000) – Unidade de Albergaria-a-Velha (faixa de cisalhamento de Porto-Tomar-Ferreira do Alentejo): principais resultados de um estudo geológico pluridisciplinar. *Geociências, Revista da Universidade de Aveiro*, **14** (1/2): 49–60.
- CHAMINÉ H. I., GAMA PEREIRA L. C., FONSECA P. E., MOÇO L. P., FERNANDES J. P., ROCHA F., FLORES D., PINTO de JESUS A., GOMES C., SOARES de ANDRADE A. A. and ARAÚJO A. (2003a) – Tectonostratigraphy of middle and upper Palaeozoic black shales from the Porto-Tomar-Ferreira do Alentejo shear zone (W Portugal): new perspectives on the Iberian Massif. *Geobios*, **36** (6): 649–663.
- CHAMINÉ H. I., GAMA PEREIRA L. C., FONSECA P. E., NORONHA F. and LEMOS de SOUSA M. J. (2003b) – Tectonoestratigrafia da faixa de cisalhamento de Porto-Albergaria-a-Velha-Coimbra-Tomar, entre as Zonas Centro-Ibérica e de Ossa-Morena (Maciço Ibérico, W de Portugal). *Cadernos Lab. Xeol. Laxe, A Coruña*, **28**: 37–78.
- CLAYTON G., COQUEL R., DOUBINGER J., GUEINN K. J., LOBOZIAK S., OWENS B. and STREEL M. (1977) – Carboniferous miospores of Western Europe: illustration and zonation. *Meded. Rijks Geol. Dienst.*, **29**: 1–71.
- COOPER A. (1980) – The stratigraphy and palaeontology of the Ordovician to Devonian rocks of the area North of Dornes (near Figueiró dos Vinhos), central Portugal. University Sheffield. Unpubl. PhD Thesis.
- COURBOULIEX S. (1974) – Étude géologique des régions de Anadia et de Mealhada: le socle, le Primaire et le Trias. *Commun. Serv. Geol., Portugal*, **58**: 5–37.
- CURTIS C. D. (1980) – Diagenetic alteration in black shales. *J. Geol. Soc. London*, **137** (2).
- De VICENTE G. and VEGAS R. (2009) – Large-scale distributed deformation controlled topography along the western Africa-Eurasia limit: tectonic constraints. *Tectonophysics*, **474**: 124–143.
- DIAS R. and RIBEIRO A. (1993) – Porto-Tomar shear zone, a major structure since the beginning of the Variscan orogeny. *Commun. Inst. Geol. Min., Portugal*, **79**: 31–40.
- DICKINSON W. R., BEACH L. S., BRACKENRIDGE G. R., ERJAVEC J. L., FERGUSON R. C., KNEPP R. A., LINDBERG F. A. and RYBERG P. T. (1983) – Provenance of North American Phanerozoic sandstones in relation to tectonic setting. *Geol. Soc. Am. Bull.*, **94**: 222–235.
- DICKINSON W. R. and SUCZEK C. A. (1979) – Plate tectonics and sandstone compositions. *Am. Ass. Petrol. Geol. Bull.*, **63** (12): 2164–2182.
- DONEGAN D. and SCHRADER H. (1982) – Biogenic and abiogenic components of laminated hemipelagic sediments in the central Gulf of California. *Mar. Geol.*, **48**: 215–237.
- ELLIN S. and McLEAN D. (1994) – The use of microwave heating in hydrofluoric acid digestions for palynological preparations. *Palynology*, **18** (1): 23–31.
- ESPITALIÉ J., DEROO G. and MARQUIS F. (1985) – La pyrolyse Rock-Eval et ses applications. *Première Partie. Rev. Inst. Franc. Pétr.*, **40** (5): 563–579.
- FERNANDES J. P., FLORES D., ROCHA F., GOMES C., GAMA PEREIRA L. C., FONSECA P. E. and CHAMINÉ H. I. (2001) – Devonian and Carboniferous palynomorph assemblages of black shales from the Ovar-Albergaria-a-Velha-Coimbra-Tomar (W Portugal): tectonostratigraphic implications for the Iberian Terrane. *Geociências, Revista da Universidade de Aveiro*, **15**: 1–23.
- FERNÁNDEZ F. J., CHAMINÉ H. I., FONSECA P. E., MUNHÁ J., RIBEIRO A., ALLER J., FUERTES-FUENTE M. and SODRÉ BORGES F. (2003) – HT-fabrics in garnet-bearing quartzite from Western Portugal: geodynamic implications for the Iberian Variscan Belt. *Terra Nova, Blackwell Publishing, Ltd.*, **15**: 96–103, doi: 10.1046/j.1365-3121.2003.00472.x
- FLORES D., GAMA PEREIRA L. C., RIBEIRO J., PINA B., MARQUES M. M., RIBEIRO M. A., BOBOS I. and PINTO de JESUS A. (2010) – The Buçaco Basin (Portugal): organic petrology and geochemistry study. *Internat. J. Coal Geol.*, **81** (4): 281–286.
- FOLK R. L. (1951) – Stages of textural maturity in sedimentary rocks. *J. Sediment. Petrol.*, **21**: 127–130.
- GAMA PEREIRA L. C. (1987) – Tipologia e evolução da sutura entre a Zona Centro Ibérica e a Zona Ossa Morena no sector entre Alvaiázere e Figueiró dos Vinhos (Portugal Central). Universidade de Coimbra, Unpubl. PhD Thesis.
- GAMA PEREIRA L. C. (1998) – A faixa de cisalhamento Porto-Tomar, no sector entre o Espinhal e Alvaiázere (Portugal Central). In: *Geólogos* (eds. H. I. Chaminé *et al.*). *Rev. Dept. Geol. Univ., Porto*, **2**: 23–27.
- GAMA PEREIRA L. C., PINA B., FLORES D. and RIBEIRO M. A. (2008) – Tectónica distensiva: o exemplo da Bacia Permo-Carbónica do Buçaco. In: *Conferência Internacional Geociências no Desenvolvimento das Comunidades Lusófonas. Mem. Not., Coimbra, N. S.*, **3**: 199–205.
- GOMES A. (2008) – Evolução geomorfológica da plataforma litoral entre Espinho e Águeda. University Porto. Unpubl. PhD Thesis.
- GOMES A., CHAMINÉ H. I., TEIXEIRA J., FONSECA P. E., GAMA PEREIRA L. C., PINTO de JESUS A., PÉREZ-ALBERTI A., ARAÚJO M. A., COELHO A., SOARES de ANDRADE A. and ROCHA F. (2007) – Late Cenozoic basin opening in relation to major strike-slip faulting along the Porto-Coimbra-Tomar fault zone (northern Portugal). In: *Sedimentary Processes, Environments and Basins: a Tribute to Peter Friend* (eds. G. Nichols, E. Williams and C. Paola). *Internat. Ass. Sediment., Spec. Pubs.*, **38**: 137–153.
- GRADSTEIN F. M., OGG J. G. and SMITH A. G., eds. (2004) – *A Geologic Time Scale 2004*. Cambridge University Press.
- HILLIER S. and MARSHALL J. (1988) – A rapid technique to make polished thin sections of sedimentary organic matter concentrates. *J. Sediment. Petrol.*, **58**: 754–755.
- INGERSOLL R. V., FULLARD T. F., FORD R. L., GRIMM J. P., PICKLE J. D. and SARES S. W. (1984) – The effect of grain size on detrital modes: a test of the Gazzi-Dickinson point-counting method. *J. Sediment. Res.*, **54** (1): 103–116.
- LAFARGUE E., MARQUIS F. and PILLOT D. (1998) – Rock-Eval 6 applications in hydrocarbon exploration, production, and soil contamination studies. *Oil and Gas Sc. Technol., Rev. IFP*, **53** (4): 421–437.
- LEFORT J. P. and RIBEIRO A. (1980) – La faille Porto-Badajoz-Cordoue a-t-elle contrôlé l'évolution de l'océan paleozoïque sud-armoricain? *Bull. Soc. Géol. France*, **22** (3): 455–462.
- MACHADO G. (2010) – Upper Palaeozoic stratigraphy and palynology of Ossa-Morena Zone, NW and SW Portugal. University of Aveiro. Unpubl. PhD Thesis.

- McCANN T. (1991) – Petrological and geochemical determination of provenance in the southern Welsh Basin. In: *Developments in Sedimentary Provenance Studies* (eds. A. C. Morton, S. P. Todd and P. D. W. Haughton). *Geol. Soc. Spec. Publ.*, **57**: 215–230.
- MEDINA J., RODRIGUEZ ALONSO M. D. and BERNARDES C. A. (1989) – Litoestratigrafia e estrutura do complexo xisto-grauváquico na região do Caramulo, Portugal. *Geociências, Revista da Universidade de Aveiro*, **4** (1): 51–73.
- MEDINA J., TASSINARI C. C. and PINTO M. S. (1993) – Idades Rb-Sr no complexo xisto-grauváquico na região de Mortágua, Portugal Central. In: *Actas IX Semana de Geoquímica e II Congresso de Geoquímica dos Países de Língua Portuguesa* (eds. F. Noronha, M. Marques and P. Nogueira): 399–403. Faculdade de Ciências da Universidade do Porto.
- MILLER M. A. (1996) – Chitinozoa. In: *Palynology: Principles and Applications* (eds. J. Jansonius and D. C. McGregor). *Am. Ass. Strat. Palynol. Found.*, **1**: 307–336.
- MOÇO L. P., CHAMINÉ H. I., FERNANDES J. P., LEMOS de SOUSA M. J., FONSECA P. E. and RIBEIRO A. (2001) – Organic metamorphism level of Devonian black shale from Albergaria-a-Velha region (NW Portugal): tectonostratigraphic implications. *Gaia*, **16**: 195–197.
- MUTTI E. and NORMARK W. R. (1987) – Comparing examples of modern and ancient turbidite systems: problems and concepts. In: *Marine Clastic Sedimentology: Concepts and Case Studies* (eds. J. K. Leggett and G. G. Zuffa): 1–38. Graham and Trotman, London.
- OBUKHOVSKAYA T. G., AVKHIMOVITCH V. I., STREEL M. and LOBOZIAK S. (2000) – Miospores from the Frasnian-Famennian boundary deposits in Eastern Europe (the Pripyat Depression, Belarus and the Timan-Pechora Province, Russia) and comparison with Western Europe (Northern France). *Rev. Palaeobot. Palynol.*, **112** (4).
- OBUKHOVSKAYA V. Y. and OBUKHOVSKAYA T. G. (2008) – Miospores of the genus *Kedoesporis* gen. nov. from Devonian deposits of Belarus (in Russian). *Lithosphere*, **2** (29): 61–65.
- OLIVEIRA J. T., PEREIRA E., PIÇARRA J. M., YOUNG T. and ROMANO M. (1992) – O Paleozóico Inferior de Portugal: síntese da estratigrafia e da evolução paleogeográfica. In: *Paleozóico Inferior de Ibero-América* (eds. J. G. Gutiérrez Marco, J. Saavedra and I. Rábano): 359–375. Universidad de Extremadura.
- PALAIN C. (1976) – Une série détritique terrigène. Les “grès de Silves”: Trias et Lias Inférieur du Portugal. *Mem. Serv. Geol., Portugal (NS)*, **25**.
- PARIS F. (1981) – Les chitinozoaires dans le Paleozoïque du SW de l’Europe. *Mem. Soc. Géol. Min. Bretagne*, **26**.
- PEREIRA E., ROMÃO J. and CONDE L. N. (1998) – Geologia da transversal de Tomar-Mação: sutura entre a Zona Centro Ibérica (ZCI) e Zona de Ossa-Morena (ZOM). In: *Livro Guia das Excursões do V Congresso Nacional de Geologia, Lisbon, Portugal* (eds. J. T. Oliveira and R. Dias): 159–188.
- PINTO de JESUS A., LEMOS de SOUSA M. J., CHAMINÉ H. I., DIAS R., FONSECA P. E. and GOMES A. (2010) – O Carbonífero em Portugal. In: *Ciências Geológicas: Ensino e Investigação e sua História. Volume I* (eds. J. M. Cotelto Neiva *et al.*): 341–355. Geologia Clássica. Ass. Portuguesa Geól./Soc. Geol., Portugal.
- POTONIÉ R. (1958) – Synopsis der Gattungen der Sporae dispersae. II. Teil: Sporites (Nachträge), Saccites, Aletes, Praecolpates, Polyplicates, Monocolpates. *Beihefte Geol. Jahrb.*, **31**.
- POTONIÉ R. (1970) – Synopsis der Gattungen der Sporae dispersae V. Nachträge zu allen Gruppen (Turmae). *Beihefte Geol. Jahrb.*, **87**: 1–22.
- PROTHERO D. R. and SCHWAB F. (1996) – Sedimentary geology. An introduction to sedimentary rocks and stratigraphy. W. H. Freeman and Company.
- RIBEIRO C. (1853) – On the Carboniferous and Silurian formations of the neighbourhood of Bussaco in Portugal (with notes and a description of the animal remains by D. Sharpe, J. W. Salter and T. Rupert Jones, and an account of the vegetable remains by Charles J. F. Bunbury). *Quart. J. Geol. Soc., London*, **9** (1–2): 135–160.
- RIBEIRO A., MUNHÁ J., DIAS R., MATEUS A., PEREIRA E., RIBEIRO M. L., FONSECA P. E., ARAÚJO A., OLIVEIRA J. T., ROMÃO J., CHAMINÉ H. I., COKE C. and PEDRO J. C. (2007) – Geodynamic evolution of SW Europe Variscides. *Tectonics*, **26** (6): TC6009.
- RIBEIRO A., MUNHÁ J., FONSECA P. E., ARAÚJO A., PEDRO J., MATEUS A., TASSINARI C., MACHADO G. and JESUS A. (2010) – Variscan Ophiolite Belts in the Ossa-Morena Zone (Southwest Iberia): geological characterization and geodynamic significance. *IGCP Project 497, Ocean Rheic Spec. Vol., Gondwana Res.* doi: 10.1016/j.gr.2009.09.005
- RIBEIRO A., PEREIRA E. and SEVERO GONÇALVES L. (1980) – Análise da deformação da zona de cisalhamento Porto-Tomar na Transversal de Oliveira de Azeméis. *Com. Inst. Geol. Min., Portugal*, **66**: 3–9.
- RICHARDSON J. B. and MCGREGOR D. C. (1986) – Silurian and Devonian spore zones of the Old Red Sandstone continent and adjacent regions. *Bull. Geol. Surv., Canada*, **365**.
- RIEGEL W. (2008) – The Late Palaeozoic phytoplankton blackout: artefact or evidence of global change. *Rev. Palaeobot. Palynol.*, **148** (2–4): 73–90.
- SEVERO GONÇALVES L. (1974) – Geologie und petrologie des Gebietes von Oliveira de Azeméis und Albergaria-a-Velha (Portugal). *Freien Universität Berlin. Unpubl. PhD Thesis*.
- STETS J. and SCHÄFER A. (2008) – The Early Devonian Rhenohercynian Basin (Middle Rhine Valley, Rheinisches Schiefergebirge). In: *The Rheno-Hercynian, Mid-German Crystalline and Saxo-Thuringian Zones (Central European Variscides)* (eds. P. Königshof and U. Linnemann): 16–54. *Excurs. Guide. Final Meet. International Geological Correlation Program (IGCP) 497 and IGCP 499. Frankfurt–Dresden, Germany*.
- STREEL M., HIGGS K., LOBOZIAK S., RIEGEL W. and STEEMANS P. (1987) – Spore stratigraphy and correlation with faunas and floras in the type marine Devonian of the Ardenne-Rhenish regions (Europe). *Rev. Palaeobot. Palynol.*, **50** (3): 211–229.
- STROTHER P. K. (2008) – A speculative review of factors controlling the evolution of phytoplankton during Paleozoic time. *Rev. Micropaleont.*, **51** (1): 9–21.
- TISSOT B. P. and WELTE D. H. (1984) – Petroleum formation and occurrence, 2nd edn. Springer, Berlin–Heidelberg–New York.
- TRAVERSE A. (2007) – Paleopalynology (2nd edition). *Topics in Geobiology* (eds. N. Landman and D. Jones). Springer, Dordrecht, The Netherlands.
- TYSON R. V. (1987) – The genesis and palynofacies characteristics of marine petroleum source rocks. *Geol. Soc. London, Spec. Publ.*, **26** (1): 47–67.
- TYSON R. V. (1993) – Palynofacies analysis. In: *Applied Micropaleontology* (ed. D. G. Jenkins): 153–191. Kluwer Acad. Publ., Dordrecht.
- VÁZQUEZ M., ABAD I., JIMÉNEZ-MILLÁN J., ROCHA F., FONSECA P. E. and CHAMINÉ H. I. (2007) – Prograde epizonal clay mineral assemblages and retrograde alteration in tectonic basins controlled by major strike-slip zones (W Iberian Variscan Chain). *Clay Miner.*, **42** (1): 109–128.
- WAGNER R. H., LEMOS de SOUSA M. J. and SILVA F. G. (1983) – Stratigraphy and fossil flora of the Upper Stephanian C of Buçaco, north of Coimbra (Portugal). In: *Contributions to the Carboniferous Geology and Palaeontology of the Iberian Peninsula* (ed. M. J. Lemos de Sousa): 127–156. Univ. Porto, Fac. Ciências, Miner., Geol., Porto.

APPENDIX A

Systematic Palynology

The turmal division used here is modified from Potonié (1958, 1970) in Traverse (2007) with additional subturmal divisions

- Anteturma SPORITES Potonié, 1893
- Turma TRILETES (Reinsch) Dettmann, 1963
- Subturma AZONOTRILETES (Luber) Dettmann, 1963
- Infraturma LAEVIGATI (Bennie and Kiston) Potonié, 1956
- Genus *Leiotriletes* (Naumova) Ischenko, 1952
Leiotriletes aff. *balapucensis* di Pasquo, 2007
Leiotriletes cf. *devonicus* Naumova, 1953
Leiotriletes aff. *devonicus* Naumova, 1953
Leiotriletes inermis (Waltz) Ischenko, 1952
Leiotriletes cf. *microgranulatus* Playford, 1962
Leiotriletes ornatus Ischenko, 1956
Leiotriletes aff. *pagius* Allen, 1965 (Fig. 5Q)
Leiotriletes aff. *trivialis* Naumova, 1953
Leiotriletes spp.
- Genus *Punctatisporites* (Ibrahim) Potonié and Kremp, 1954
Punctatisporites cf. *glaber* (Naumova) Playford, 1962
Punctatisporites minutus Kosanke, 1950 (Fig. 7O)
Punctatisporites irrasus Hacquebard, 1957
Punctatisporites lucidulus Playford and Helby, 1968
Punctatisporites planus Hacquebard, 1957
Punctatisporites cf. *reticulopunctatus* Hoffmeister, Staplin and Malloy, 1955
Punctatisporites sol i du Hacquebard, 1957
Punctatisporites springsurensis Playford, 1978
Punctatisporites spp.
- Genus *Retusotriletes* (Naumova) Streele, 1964
Retusotriletes cf. *communis* Naumova, 1953 (Fig. 5T)
Retusotriletes cf. *dubius* (Eisenack) Richardson, 1965
Retusotriletes incohatus Sullivan, 1964
Retusotriletes mi nor Kedo, 1963 (Fig. 5U)
Retusotriletes cf. *pychovii* Naumova, 1953
Retusotriletes cf. *scabratus* Turnau, 1986
Retusotriletes warringtonii Richardson and Lister, 1969 (Fig. 5X)
Retusotriletes spp.
- Infraturma APICULATI (Bennie and Kidston) Potonié, 1956
- Subinfraturma GRANULATI Dybová and Jachowicz, 1957
- Genus *Cyclogranisporites* Potonié and Kremp, 1954
Cyclogranisporites sp.
- Genus *Geminospora* Balme, 1952
Geminospora cf. *aurita* Arkhangelskaya, 1985 (Fig. 5I)
Geminospora lemurata Balme, 1962 (Fig. 5J)
Geminospora micromanifesta (Naumova) Arkhangelskaya, 1985 (Fig. 5K)
- REMARKS. – The distinction between *G. lemurata* and *G. micromanifesta* seems to rely solely on fine details of the ornamentation which are very similar. It is likely that these two species are conspecific. The preservation of the present material does not allow a detailed study of this topic.
- Geminospora notata* (Naumova) Obukhovskaya, 1993 (Fig. 5L)
Geminospora spp.
- Genus *Granulatisporites* (Ibrahim) Schopf, Wilson, and Bentall, 1944
Granulatisporites sp.
- Genus *Tricidarisporites* Sullivan and Marshall, 1966
Tricidarisporites fasciculatus (Love) Sullivan and Marshall, 1966
- Subinfraturma VERRUCATI Dybová and Jachowicz, 1957
- Genus *Grumosisporites* Smith and Butterworth, 1967
Grumosisporites inaequalis (Butterworth and Williams) Smith and Butterworth, 1967 (Fig. 8AA)
Grumosisporites cf. *verrucosus* (Butterworth and Williams) Smith and Butterworth, 1967
Grumosisporites sp. (Fig. 8BB)
- Genus *Verrucosisporites* (Ibrahim) Smith, 1971
Verrucosisporites baccatus Staplin, 1960 (Fig. 8L)
Verrucosisporites nitidus morphon (*sensu* Van der Zwan, 1980)
Verrucosisporites tumultentus Clayton and Graham, 1974
Verrucosisporites cf. *scurrus* (Naumova) McGregor and Camfield, 1982 (Fig. 9I)
Verrucosisporites spp.
- Subinfraturma NODATI Dybová and Jachowicz, 1957
- Genus *Acanthotriletes* (Naumova) Potonié and Kremp, 1954
Acanthotriletes cf. *aculeolatus* (Kosanke) Potonié and Kremp, 1955 (Fig. 8N)
Acanthotriletes aff. *echinatus* Hoffmeister, Staplin and Malloy, 1955 (Fig. 8O)
Acanthotriletes spp.
- Genus *Aneurospora* (Streele) Richardson, Streele, Hassan and Steemans, 1982
Aneurospora (*Geminospora*) *extensa* morphon (*A. extensa*-*A. goensis*) Turnau, 1999 (Fig. 5A, B)
Aneurospora cf. *greggsii* (McGregor) Streele, 1974 (Fig. 5C)
Aneurospora sp.
- Genus *Apiculatisporis* (Ibrahim) Potonié and Kremp, 1956
Apiculatisporis cf. *porosus* Williams in Neves *et al.*, 1973 (Fig. 8Q)
Apiculatisporis cf. *hacquebardi* Playford, 1964 (Fig. 8A, A')
Apiculatisporis cf. *variocorneus* Sullivan, 1964 (Fig. 8R)
Apiculatisporis spp.
- Genus *Apiculatisporites* Potonié and Kremp, 1956
Apiculatisporites davenportensis Peppers, 1969
Apiculatisporites wapsipiniconensis Peppers, 1969
Apiculatisporites sp.
- Genus *Apiculiretusispora* (Streele) Streele, 1977
Apiculiretusispora cf. *arenorugosa* McGregor, 1973
Apiculiretusispora cf. *gaspensis* McGregor, 1973
Apiculiretusispora cf. *perfectae* Steemans, 1989 (Fig. 5V)
Apiculiretusispora cf. *plicata* (Allen) Streele, 1967
Apiculiretusispora cf. *synorea* Richardson and Lister, 1969
Apiculiretusispora spp.
- Genus *Grandispora* (Hoffmeister, Staplin and Malloy) McGregor, 1973
Grandispora aff. *cornuta* Higgs, 1975 (Fig. 7L)
Grandispora cf. *echinata* Hacquebard, 1957 (Fig. 7K)
Grandispora cf. *famenensis* (Naumova) Streele, 1974 in Becker *et al.* 1974 var. *minuta* Nekriata, 1974 (Fig. 7M)
Grandispora gracilis (Kedo) Streele in Becker *et al.*, 1974 (Fig. 7N)
Grandispora cf. *gracilis* (Kedo) Streele in Becker *et al.*, 1974 (Fig. 8M)
Grandispora cf. *miconulata* (Kedo) Avkhimovitch, 2000
aff. *Grandispora microseta* (Kedo) Streele in Becker *et al.*, 1974
Grandispora minuta (Kedo) Avkhimovitch, 2000
Grandispora permulta (Daemon) Loboziak, Streele and Melo, 1999
Grandispora tamarae Loboziak in Higgs *et al.*, 2000
Grandispora aff. *tamarae* Loboziak in Higgs *et al.*, 2000 (Fig. 9J)

Grandispora aff. *velata* (Eisenack) McGregor, 1973 (Fig. 9N)
Grandispora spp.

Genus *Lophotriteles* (Naumova) Potonié and Kremp, 1954
Lophotriteles atratus Naumova, 1953
aff. *Lophotriteles multififormis* Tchibrikova, 1977 (Fig. 5S)
Lophotriteles sp.

Genus *Spinozonotriteles* (Hacquebard) Neves and Owens, 1966
Spinozonotriteles sp.

Subinfraturma BACULATI Dybová and Jachowicz, 1957

Genus *Ancyrospora* Richardson, 1960
cf. *Ancyrospora? andevalensis* González, Playford
and Moreno, 2005 (Fig. 8P)
Ancyrospora sp.

Genus *Raistrickia* (Schopf, Wilson and Bentall) Potonié and Kremp, 1954
Raistrickia im bri cat Kosanke, 1950
Raistrickia sp.

Infraturma MURORNATI Potonié and Kremp, 1954

Genus *Acinosporites* Richardson, 1965
Acinosporites sp.

Genus *Convolutispora* Hoffmeister, Staplin and Malloy, 1955
Convolutispora cf. *ampla* Hoffmeister, Staplin and Malloy, 1955 (Fig. 8S)
Convolutispora cf. *re br* Butterworth and Williams, 1958 (Figs. 7A and 8T)
Convolutispora cf. *ce re br* Butterworth and Williams, 1958
Convolutispora circumvallata Clayton, 1971 (Fig. 8U)
Convolutispora aff. *disparalis* Allen, 1965 (Fig. 8V)
Convolutispora florida Hoffmeister, Staplin and Malloy, 1955
Convolutispora jugosa Smith and Butterworth, 1967
Convolutispora paraverrucata McGregor, 1964 (Fig. 7C)
Convolutispora subtilis Owens, 1971 (Figs. 7B and 8W)
Convolutispora varicosa Butterworth and Williams, 1958 (Fig. 7D)
Convolutispora cf. *vermiformis* Hughes and Playford, 1961 (Fig. 7E)
Convolutispora spp. (e.g., Fig. 7F)

Genus *Corbulispora* Bharadwaj and Venkatachala, 1961
Corbulispora cancellata (Waltz) Bharadwaj and Venkatachala, 1961
(Fig. 7G)

Genus *Cordylosporites* Playford and Satterthwait, 1985
Cordylosporites sp.

Genus *Dictyotriteles* (Naumova) Smith and Butterworth, 1967
Dictyotriteles cf. *aequalis* Staplin, 1960 (Fig. 8Y)
Dictyotriteles castaneaeformis (Horst) Sullivan, 1964 (Fig. 8Z)
Dictyotriteles cf. *densoreticulatus* Potonié and Kremp, 1955
Dictyotriteles submarginatus (Playford) Van der Zwan, 1980 (Fig. 7I)
Dictyotriteles spp.

Genus *Emphanisporites* McGregor, 1961
Emphanisporites rotatus (McGregor) McGregor, 1973 (Fig. 7J)
Emphanisporites sp.

Genus *Microreticulatisporites* (Knox) Potonié and Kremp, 1954
Microreticulatisporites concavus Butterworth and Williams, 1958

Genus *Rugospora* Neves and Owens, 1966
Rugospora cf. *flexuosa* (Jushko) Streef
in Becker *et al.*, 1974 (Figs. 7P and 9M)
Rugospora polyptycha Neves and Ioannides, 1974
Rugospora spp.

Suprasubturma CAVATITRILETES

Subturma ZONOCAVATITRILETES

Genus *Kedoesporis* (Naumova) Obukhovskaya and Obukhovskaya, 2008
Kedoesporis imperfectus (Naumova) Obukhovskaya and Obukhovskaya,
2008 (Fig. 5P)

Subturma ZONOTRILETES Waltz, 1935

Genus *Triquitrites* Wilson and Coe, 1940
Triquitrites aff. *bucculentus* Guennel, 1958
Triquitrites spp. (e.g., Fig. 8K)

Infraturma CINGULATI (Potonié and Klaus) Dettmann, 1963

Genus *Archaeozonotriteles* (Naumova) Allen, 1965
Archaeozonotriteles chulus cf. var. *chulus* (Cramer) Richardson
and Lister, 1969
aff. *Archaeozonotriteles divellomedium* (Chibrikova) Burgess
and Richardson, 1991
Archaeozonotriteles sp.

Genus *Camptozonotriteles* Staplin, 1960
Camptozonotriteles cf. *verrucosus* Butterworth and Williams, 1958

Genus *Contagisporites* Owen, 1971
Contagisporites optivus var. *vorobjevensis* (Chibrikova)
Owens, 1971 (Fig. 5F)

Genus *Knoxisporites* (Potonié and Kremp) Neves, 1961
Knoxisporites concentricus (Byvsheva) Playford and McGregor, 1993
Knoxisporites aff. *concentricus* (Byvsheva) Playford and McGregor, 1993
Knoxisporites ruhlandii Doubinger and Rauscher, 1966
Knoxisporites cf. *ruhlandii* Doubinger and Rauscher, 1966
Knoxisporites cf. *triradiatus* Hoffmeister, Staplin and Malloy, 1955
Knoxisporites spp. (e.g., Fig. 7E)

Genus *Lophozonotriteles* (Naumova) Potonié, 1958
Lophozonotriteles cf. *Convolutispora insulosa* Playford, 1978
Lophozonotriteles bellus Kedo, 1963
Lophozonotriteles cf. *bouckaertii* Loboziak and Streef, 1989
Lophozonotriteles cf. *lebedianensis* Naumova, 1953
Lophozonotriteles cf. *grandis* (Naumova) Arkhangel'skaya, 1985
Lophozonotriteles media Taugourdeau-Lantz, 1967 (Fig. 5R)
Lophozonotriteles tuberosus Sullivan, 1964
Lophozonotriteles spp. (e.g., Figs. 8F and 9L)

Genus *Savitrissporites* Bharadwaj, 1955
cf. *Savitrissporites nux* (Butterworth and Williams) Smith and Butterworth,
1967 (Fig. 9F)

Genus *Stenozonotriteles* (Naumova) Potonié, 1958
Stenozonotriteles cf. *bracteolus* (Butterworth and Williams) Smith and
Butterworth, 1967
Stenozonotriteles lycosporoides (Butterworth and Williams) Smith and
Butterworth, 1967 (Fig. 8J)
Stenozonotriteles spp.

Genus *Tumulispora* Staplin and Jansonius, 1964
aff. *Tumulispora rarituberculata* (Luber) Potonié, 1966

Subturma ZONOLAMINATITRILETES Smith and Butterworth, 1967

Infraturmae CRASSITI (Bharadwaj and Venkatachala) Smith and
Butterworth, 1967 and CINGULICAVATI Smith and Butterworth, 1967

Genus *Crassispora* (Bharadwaj) Sullivan, 1964
Crassispora aff. *kosankei* (Potonié and Kremp) Smith and Butterworth, 1967
Crassispora spp.

Genus *Cristatisporites*
Cristatisporites aff. *echinatus* Playford, 1963
aff. *Cristatisporites inaequus* (McGregor) Gao, 1975
Cristatisporites triangulatus (Allen) McGregor and Camfield, 1982 (Fig. 5G)
Cristatisporites spp.

Genus *Cristicavatispora* González, Playford and Moreno, 2005
Cristicavatispora dispersa González, Playford and Moreno, 2005

Genus *Densosporites* (Berry) Butterworth, Jansonius, Smith and Staplin, 1964
Densosporites annulatus (Loose) Smith and Butterworth, 1967 (Fig. 8D, X)
cf. *Densosporites devonicus* Richardson, 1960 (Fig. 5H)
Densosporites spinifer Hoffmeister, Staplin and Malloy, 1955
Densosporites spp.

Genus *Hymenozonotriteles* (Naumova) Potonié, 1958
Hymenozonotriteles cristatus Menendez and Pöthe de Baldi, 1967 (Fig. 5O)
Hymenozonotriteles cf. *cristatus* Menendez, 1967
Hymenozonotriteles (*Samarisporites*) cf. *inaequus* (McGregor) Owens, 1971
Hymenozonotriteles cf. *incisus* Naumova, 1953
Hymenozonotriteles spp. (Fig. 7R–T)

Genus *Lycospora* (Schopf, Wilson and Bentall) Potonié and Kremp, 1954
Lycospora cf. *subtriquetra* (Luber) Potonié and Kremp, 1956 (Fig. 9C)
Lycospora spp. (e.g., Fig. 8G)

Genus *Samarisporites* Richardson, 1965
Samarisporites spp. (e.g., Fig. 9N)

Infraturma PATINATI (Butterworth and Williams) Playford and Dettman, 1996

Genus *Chelinospora* Allen, 1965
Chelinospora concinna Allen, 1965 (Fig. 5E)
Chelinospora spp.

Genus *Camarozonotriletes* (Naumova) Naumova, 1953
Camarozonotriletes cf. *antiquus* (Naumova) Kedo, 1955
Camarozonotriletes spp.

Genus *Cymbosporites* Allen, 1965
Cymbosporites cyathus Allen, 1965
Cymbosporites sp.

Genus *Cyrtozpora* Winslow, 1962
Cyrtozpora cristifer (Luber) Van der Zwan, 1979 (Fig. 7H)

Supersubturma PSEUDOSACCITRILETES Richardson, 1965

Infraturma MONOPSEUDOSACCITI Smith and Butterworth, 1967

Genus *Auroraspora* Hoffmeister, Staplin and Malloy, 1955
Auroraspora cf. *asperella* (Kedo) Van der Zwan, 1980
Auroraspora asperella variant B (Kedo) Van der Zwan, 1979 (Fig. 7D)
Auroraspora micromanifesta (Hacquebard) Richardson, 1960
Auroraspora spp.

Genus *Diducites* Van Veen, 1981
Diducites sp.

Genus *Spelaotriletes* Neves and Owens, 1966
 aff. *Spelaotriletes balteatus* (Playford) Higgs, 2006

Subturma PERINOTRILETES Erdtman, 1947

Genus *Perotriletes* (Erdtman) Couper, 1953
 aff. *Perotriletes tessellatus* (Staplin) Neville in Neves *et al.*, 1973
Perotriletes sp.

Genus *Propriisporites* Neves, 1958
Propriisporites laevigatus Neves, 1961 (Fig. 9D)

Turma MONOLETES Ibrahim, 1933

Subturma AZONOMONOLETES Luber, 1935

Infraturma LAEVIGATOMONOLETI Dybová and Jachowicz, 1957

Genus *Laevigatosporites* (Ibrahim) Schopf, Wilson and Bentall, 1944
Laevigatosporites spp. (Fig. 8CC)

Genus *Latosporites* Potonié and Kremp, 1954
Latosporites cf. *ovalis* Breuer, Al-Ghazi, Al-Ruwaili, Higgs, Steemans and Wellman, 2007 (Fig. 5Y)
Latosporites sp.

Anteturma POLLENITES Potonié, 1931

Turma SACCITES Erdtman, 1947

Subturma MONOSACCITES Potonié and Kremp, 1954

Infraturma TRILETESACCITI Leschik, 1955

Genus *Schulzospora* Kosanke, 1950
Schulzospora spp. (Fig. 8I)

Infraturma VESICULOMONORADITI Pant, 1954

Archaeoperisaccus aff. *ovalis* Naumova, 1953 (Fig. 7Q)

INCERTAE SEDIS

Genus *Corystisporites* Richardson, 1965
Corystisporites sp.

Genus *Radialetes* Playford, 1963
 aff. *Radialetes* sp. (Fig. 9F)

APPENDIX B

Rock-Eval parameters of the analysed samples from the AVU

Sample	T _{max} [°C]	S1 [mgHC/g rock]	S2 [mgHC/g rock]	S3 [mgCO ₂ /g rock]	PI S1/(S1+S2)	S4 CO ₂ [mgCO ₂ /g rock]	S4 CO [mgCO/g rock]	S5 [mgCO ₂ /g rock]
ANG16	422	0.04	0.05	0.04	0.44	6.2	1.1	4
VAL4	354	0.03	0.05	0.07	0.38	4.3	0.2	3
MIN16.3	333	0.04	0.04	0.13	0.50	1.2	0.6	3
LOB1.1	329	0.02	0.02	0.02	0.50	11.5	2.8	3
MIR4.3	337	0.03	0.02	0.09	0.60	2.3	0.3	3
CAT5.1	353	0.05	0.04	0.08	0.57	9.4	1.9	2
CHE1.1	343	0.02	0.04	0.13	0.33	5.7	2.0	3
ALH1.4	324	0.04	0.05	0.09	0.44	2.1	0.8	2
SAL3.1	328	0.01	0.01	0.00	0.50	6.0	2.6	9
GOL1.1	351	0.01	0.02	0.06	0.33	1.6	2.0	2
SER2	326	0.01	0.02	0.02	0.33	1.7	2.1	2
TRE1.1	343	0.02	0.04	0.05	0.33	1.8	2.0	4

PI – production index

Sample	PC [%]	RC [%]	TOC [%]	HI [mgHC/gTOC]	OI [mgCO ₂ /gTOC]	mineral carbon [%]	Age
ANG16	0.01	0.22	0.23	22	17	0.11	Serpukhovian
VAL4	0.01	0.13	0.14	36	50	0.12	late Famennian
MIN16.3	0.01	0.06	0.07	57	186	0.09	early Frasnian
LOB1.1	0.01	0.43	0.44	5	5	0.08	early Tournaisian
MIR4.3	0.01	0.07	0.08	25	113	0.08	?
CAT5.1	0.01	0.34	0.35	11	23	0.06	Visean
CHE1.1	0.01	0.25	0.26	15	50	0.10	early Visean
ALH1.4	0.01	0.09	0.10	50	90	0.15	?
SAL3.1	0.01	0.27	0.28	4	0	0.25	?
GOL1.1	0.01	0.13	0.14	14	43	0.15	?
SER2	0.01	0.14	0.15	13	13	0.06	Serpukhovian
TRE1.1	0.01	0.14	0.15	27	33	0.11	?

PC – pyrolyzable organic carbon, RC – residual carbon organic

APPENDIX C

Localities details

Locality code	Locality (nearest village)	Age	Deformation	Number of samples	Analysis successfully performed		
					Palynology	Rock-Eval	Detrital framework
AM11	Sernada	Serpukhovian	heavy	1	X		
FON	Font o	Serpukhovian	light	4	X		X
SER	Serém	Serpukhovian	heavy	2	X	X	
QUI	Quintinha	Serpukhovian	light	2	X		X
CAT	Catraia	Serpukhovian/Visean	medium	3	X	X	
PIC	Picoito	Visean	light	1	X		
TOR	Torres de Mondego	Visean	heavy	1	X		
FRA	S. Paulo de Frades	Visean	medium	2	X		
CHE	Cheira	early Visean	medium	2	X	X	
LOB	Lobazes	early Tournaisian	heavy	2	X	X	
BOU	Bouça	Famennian–Tournaisian	heavy	1	X		
CAN	Vale da Canas	Famennian–Tournaisian	heavy	1	X		
TAP	Tapada	Famennian–Tournaisian	heavy	1	X		
TOV	Tovim	Famennian–Tournaisian	heavy	1	X		
ASS	Assilhó	Famennian–Tournaisian	heavy	1	X		
VAL	Valmaior	late Famennian	heavy	4	X	X	
MAR	S. Marcos	Famennian–Tournaisian	heavy	1	X		
SND	Sernada do Vouga	Famennian–Tournaisian	heavy	1	X		
POR	Portos	Famennian–Tournaisian	heavy	1	X		
AUT	A29 highway (near Salreu)	Famennian–Tournaisian	heavy	1	X		
SPD	Lameira S. Pedro	Famennian–Tournaisian	heavy	1	X		
DUP	Vila Duparchy	Famennian–Tournaisian	heavy	1	X		
RET	Retorta	Frasnian	heavy	1	X		
MIN	Minhoteira	early Frasnian	heavy	6	X	X	
LUS	Luso	Frasnian	medium	1	X		
ALH	Alhandra	?	light	3		X	X
BOS	Bostelim	?	light	2			X
CND	Candam	?	light	1			X
MON	Monsarros	Serpukhovian	light	3	X		X
ZOR	Zorro	?	medium	1			X
ANG	Angeja	Serpukhovian	light	2	X	X	
MIR	Miranda do Corvo	?	medium/heavy	1		X	
SAL	Salgueiral	?	medium	1		X	
GOL	Golpe	?	heavy	1		X	
TRE	Tremoa	?	heavy	1		X	